

RESEARCH ARTICLE

10.1002/2016WR019267

Differences in behavior and distribution of permafrost-related lakes in Central Yakutia and their response to climatic drivers

M. Ulrich¹, H. Matthes², L. Schirrmeister³, J. Schütze⁴, H. Park^{5,6}, Y. Iijima⁷, and A. N. Fedorov^{8,9}

Key Points:

- Remote sensing, field, and statistical analysis of thermokarst-lake change in relation to long-term climate records and geomorphology
- Type and degree of climatic and geomorphological influence depend on lake type, size, origin, and evolution
- Thermokarst activity will remain at a high level and wet conditions within alas basins will persist in the near future

Supporting Information:

- Supporting Information S1

Correspondence to:

M. Ulrich,
Mathias.Ulrich@uni-leipzig.de

Citation:

Ulrich, M., H. Matthes, L. Schirrmeister, J. Schütze, H. Park, Y. Iijima, and A. N. Fedorov (2017), Differences in behavior and distribution of permafrost-related lakes in Central Yakutia and their response to climatic drivers, *Water Resour. Res.*, 53, doi:10.1002/2016WR019267.

Received 25 MAY 2016

Accepted 5 JAN 2017

Accepted article online 10 JAN 2017

¹Institute for Geography, Leipzig University, Leipzig, Germany, ²Atmospheric Circulations Section, Alfred Wegener Institute, Potsdam, Germany, ³Periglacial Research Section, Alfred Wegener Institute, Potsdam, Germany, ⁴Department of Fundamental Science, University of Applied Sciences Jena, Jena, Germany, ⁵Institute of Arctic Climate and Environment Research, Japan Agency for Marine-Earth Science and Technology, Yokosuka, Japan, ⁶Institute for Space-Earth Environmental Research, Nagoya University, Nagoya, Japan, ⁷Graduate School of Bioresources, Mie University, Tsu, Japan, ⁸Melnikov Permafrost Institute, SB RAS, Yakutsk, Russia, ⁹Faculty of Geology and Survey, North-Eastern Federal University, Yakutsk, Russia

Abstract The Central Yakutian permafrost landscape is rapidly being modified by land use and global warming, but small-scale thermokarst process variability and hydrological conditions are poorly understood. We analyze lake-area changes and thaw subsidence of young thermokarst lakes on ice-complex deposits (yedoma lakes) in comparison to residual lakes in alas basins during the last 70 years for a local study site and we record regional lake size and distribution on different ice-rich permafrost terraces using satellite and historical airborne imagery. Statistical analysis of climatic and ground-temperature data identified driving factors of yedoma- and alas-lake changes. Overall, lake area is larger today than in 1944 but alas-lake levels have oscillated greatly over 70 years, with a mean alas-lake-radius change rate of 1.6 ± 3.0 m/yr. Anthropogenic disturbance and forest degradation initiated, and climate forced rapid, continuous yedoma-lake growth. The mean yedoma lake-radius change rate equals 1.2 ± 1.0 m/yr over the whole observation period. Mean thaw subsidence below yedoma lakes is 6.2 ± 1.4 cm/yr. Multiple regression analysis suggests that winter precipitation, winter temperature, and active-layer properties are primary controllers of area changes in both lake types; summer weather and permafrost conditions additionally influence yedoma-lake growth rates. The main controlling factors of alas-lake changes are unclear due to larger catchment areas and sub-surface hydrological conditions. Increasing thermokarst activity is currently linked to older terraces with higher ground-ice contents, but thermokarst activity will likely stay high and wet conditions will persist within the near future in Central Yakutian alas basins.

1. Introduction and Background

In the initial phase of thermokarst evolution thaw lakes are a special focus of research, because they are sensitive to variations in climate, permafrost, vegetation, and anthropogenic land use. In addition, lake-area changes and related permafrost dynamics may influence regional hydrology, biogeochemistry, and climate, as well as human living conditions [Soloviev, 1961; Bosikov, 1998; Walter et al., 2007; Jones et al., 2011; van Huissteden et al., 2011; Grosse et al., 2013]. Modern driving factors for lake-area changes are, however, not yet well understood. Thermokarst studies have focused on ongoing lake changes during the last decades using mainly multitemporal remote-sensing data. These change-detection studies have covered mostly arctic regions [Smith et al., 2005; Plug et al., 2008; Jones et al., 2011; Olthof et al., 2015] and also boreal regions in Alaska [Yoshikawa and Hinzman, 2003; Riordan et al., 2006; Roach et al., 2011; Chen et al., 2014; Lara et al., 2016] and Central Yakutia (CY), Siberia [Kravtsova and Bystrova, 2009; Tarasenko, 2013; Boike et al., 2016]. They show thermokarst-lake areas that increase [Smith et al., 2005; Boike et al., 2016] as well as areas that decrease resulting from lake drainage and/or drying [Riordan et al., 2006; Lantz and Turner, 2015]. Stable areas where no or only small changes occurred were also found [Riordan et al., 2006; Kravtsova and Bystrova, 2009]. Often, the change of lake area is due to more complex causes, depending on the permafrost zonation (continuous versus discontinuous) and on geomorphological and cryolithological conditions. Fluctuations can be seen in lake numbers and the area of different-sized lakes on small spatial scales [Smith et al., 2005; Jones et al., 2011]. Long-term investigations on thermokarst lake-area changes mainly suggest precipitation

(P), evaporation (E), and/or water balance (P-E) as important drivers of variations in lake area [Riordan *et al.*, 2006; Plug *et al.*, 2008; Jones *et al.*, 2009; Labrecque *et al.*, 2009; Chen *et al.*, 2014]. Internal permafrost-related features (e.g., ice content and distribution, sediment properties) not controlled by modern climatic dynamics but by paleo-environmental dynamics are additional factors that may influence local thermokarst-lake formation and desiccation [Yoshikawa and Hinzman, 2003; van Huissteden *et al.*, 2011; Pestryakova *et al.*, 2012]. Furthermore, the depth and size of thermokarst lakes and their ice-cover thickness are relevant for thermokarst dynamics because these factors affect the ground thermal regime and the formation of unfrozen zones (taliks) below a lake [West and Plug, 2008; Grosse *et al.*, 2013; Arp *et al.*, 2015].

Thermokarst processes are a widespread phenomenon in the continuous permafrost regions of CY, Russia (Figure 1), linked closely to the large-scale existence of ice-rich permafrost deposits (called yedoma or ice complexes). Previous studies of lake changes in CY by Kravtsova and Tarasenko [2011], Tarasenko [2013], or Boike *et al.* [2016] reveal a general large-scale increase of lake area from the 1980s until 2009 with a considerable increase especially in 2006 and 2007, but at other times more stable conditions were found. Precipitation is suggested as the main driving factor for the observed variations but this association is not statistically proved [e.g., Tarasenko, 2013]. Furthermore, previous studies did not differentiate between different kinds of lakes with regard to their type, size, and geomorphological situation. In CY lakes mainly occur as residual lakes in large thermokarst basins (i.e., alases; here named alas lakes) and as comparatively young and rather small thaw lakes on yedoma uplands framing the alases (here named yedoma lakes; see supporting information Figure S1). Ground ice below alas lakes has thawed almost completely and the lake water balance is thought to depend entirely on precipitation and evaporation. Many Russian studies emphasize the cyclical character of CY alas-lake changes in relation to cyclical changes of climatic conditions [Soloviev, 1961; Bosikov, 1998; Desyatkin, 2004]. Ice-wedge melt supplies 25–30% of water to yedoma lakes, instead, and these lakes tend to grow continuously once initiated [Fedorov *et al.*, 2014a].

In the last two to three decades, several studies have focused on the activation and short-term dynamics of thermokarst in CY [Bosikov, 1998; Brouchkov *et al.*, 2004; Fedorov and Konstantinov, 2009; Fedorov *et al.*, 2014a], mainly associated with climate changes and anthropogenic disturbances such as forest clearance and fires [Iijima *et al.*, 2010; Fedorov *et al.*, 2014b]. Recent short-term CY thermokarst (lake) dynamics have depended mainly on vegetation types. The rate of ground-ice thawing and surface subsidence is smaller under boreal forest covering yedoma uplands due to a shallower active layer (i.e., the seasonal thaw layer). Meadows (i.e., forest-free areas) on the flat yedoma uplands result mainly from forest clearance and/or fires. The natural sensitivity of thermokarst landscapes to climatic impacts is increasingly stressed in CY by anthropogenic impacts (e.g., agricultural land use, construction activity, water reservoirs for local populations). Disturbed surfaces, where the forest was destroyed for cultivation, are most vulnerable to permafrost degradation and thaw-lake initiation [Fedorov and Konstantinov, 2009]. A small active-layer deepening could initiate thermokarst processes within just a few years if ice-rich deposits are located near the surface [Iwahana *et al.*, 2005]. Fedorov *et al.* [2014a] reported that yedoma lakes had grown fast in such disturbed areas over a period of ~15 years up to 2008, with surface subsidence rates of 17–24 cm/yr. Yedoma lakes have, thus, continuously increased in area and are expanding into formerly dry places.

Understanding alas and yedoma lake behavior and its difference in CY is essential because, on the one hand, alas lakes represent a large fraction of the local population's natural water resources and lake-area changes will impact indigenous economies, as can already be documented by local and regional experience [Crate, 2008, 2011; Mészáros, 2012], but, on the other hand, unusual yedoma lake expansion and young thermokarst phenomena may impact usable land area, needed resources, and the stability of buildings [Desyatkin, 2004; Crate, 2011]. Investigating the spatial and temporal complexity of permafrost degradation processes will thus not only help to understand factors influencing, and possible feedback mechanisms to climate and carbon cycling; it is also important for evaluating and estimating future landscape evolution and the impacts on human land use and livelihood. Starting from the assumption that alas and yedoma lakes (the latter resulting mainly from forest clearance and/or fires) react differently to changes in climate and permafrost conditions, the objectives of this study were (1) to explore geomorphological lake characteristics and to quantify rates of alas and yedoma lake-area changes during different periods since the 1940s with estimation of surface subsidence on local scales; (2) to identify climatological and/or general driving and inducing factors by comparing yedoma- and alas-lake growth and changes through the application of statistical methods; (3) to analyze size and distribution of lakes >0.1 ha on geomorphologically different

ice-rich permafrost terraces in the Lena-Aldan interfluvium region as a basis for further change-detection studies on regional scales; and (4) to discuss possible geo-ecological and socioeconomic implications for permafrost landscape evolution and land use in CY.

2. Regional Setting

CY is located in the zone of continuous permafrost with permafrost depths reaching several hundred meters (Figure 1). The active layer reaches depths of 1.0 m below forest and up to 2.0 m in grassland areas. Taliks usually exist only below beds of major rivers and below lakes whose depths exceed that of winter-ice thickness. The ice thickness was measured in spring 2015 at several yedoma and alas lakes to average between 0.7 and 0.8 m. The region is characterized by a strong continental climate with low annual precipitation of 223 ± 54 mm and a mean annual air temperature (MAAT) of $-9.8 \pm 1.8^\circ\text{C}$, both calculated from Yakutsk weather stations' 1910–2014 data records [NOAA/NCDC, 2015]. The annual air temperature range can be $> 60^\circ\text{C}$ and annual evaporation usually exceeds annual precipitation; summer precipitation is higher than winter precipitation. Winters are long and cold and the area is snow-covered from the end of September/early October until May. Subsurface temperatures in the region at 10–15 m depth usually range from

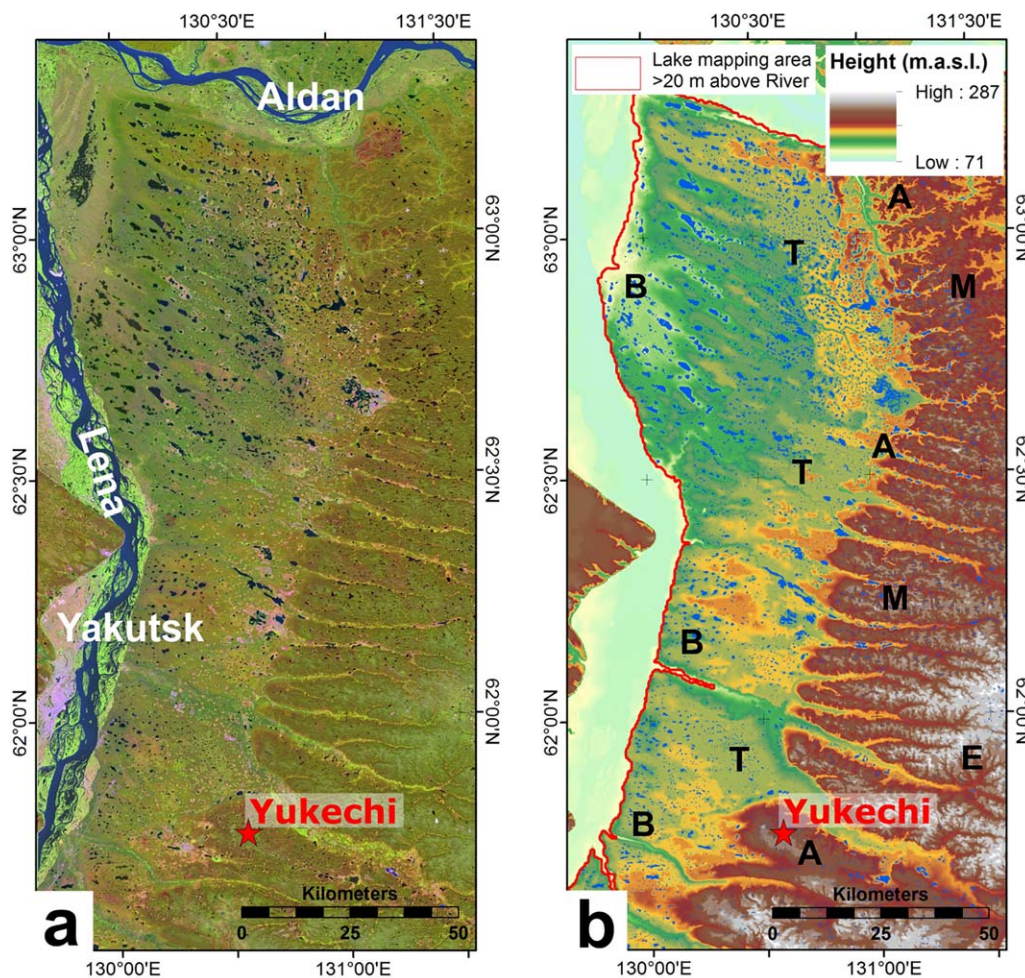


Figure 1. Study area in CY, Russia, and its main characteristics. (a) Thermokarst landscape within the Lena-Aldan interfluvium region. The main Yukechi study site is highlighted by the red star (Landsat 8 closeup, July 2013, USGS). (b) The topography of the Lena-Aldan interfluvium region showing the different Pleistocene accumulative-erosive terraces following Soloviev [1959]. B: Bestyakh terrace (56–78 m a.r.l.), T: Tyungyulyu terrace (65–100 m a.r.l.), A: Abalakh terrace (115–135 m a.r.l.), M: Magan terrace (~156 to 176 m a.r.l.), E: Emilsk terrace (194–212 m a.r.l.). In particular the Tyungyulyu and the Abalakh terraces are differentiated due to characteristics and distribution of ice-rich permafrost deposits. (Digital Elevation Model (DEM) generated using data from the European Space Agency (ESA) Data User Element (DUE) Permafrost Project [Santoro and Strozzi, 2012]).

about -3°C below dense forest cover to about -2°C below meadow areas [Fedorov *et al.*, 2014b]. Vegetation in CY is typically dominated by larch, pine, and birch forest. Alas basins form islands of grasslands therein dominated by steppe-like to swampy communities, depending on hydrologic and edaphic factors [Mirkin *et al.*, 1985; Desyatkin, 2008].

CY is bounded by the large Lena and Aldan rivers. Major parts of this interfluvial region are covered by ice-rich silty loam containing up to 80 vol% of ice, mainly existing as huge syngenetic ice wedges. These ice-complex deposits form the yedoma uplands that surround alas basins [Soloviev, 1973]. Five terraces are geomorphologically distinguished with regard to ice-complex accumulation and degradation (Figure 1) [Soloviev, 1959, 1973]. On the lowest Bestyakh terrace ice-rich deposits and, therefore, thermokarst features are almost absent due to the widespread existence of sandy soils. On the highest Magan and Emilsk terraces, a ~ 6 to 15 m-thick ice-complex cover connected to thermokarst is restricted to some valleys. Typical well-developed alas basins and many thermokarst landforms are found mainly on the Tyungyulyu and Abalakh terraces. Both terraces are characterized by thick ice-rich deposits (>25 m in some places) but they show different ages, cryolithological conditions, and characters of thermokarst landforms [Soloviev, 1959].

The Yukechi study site is located about 50 km southeast from Yakutsk on the Abalakh terrace (Lat: 61.76128° , Long: 130.47060° , Height: 210 – 218 m a.s.l.). It is a typical CY alas landscape, settled by Sakha pastoralists and monitored for several decades by the Melnikov Permafrost Institute in Yakutsk [Bosikov 1998;

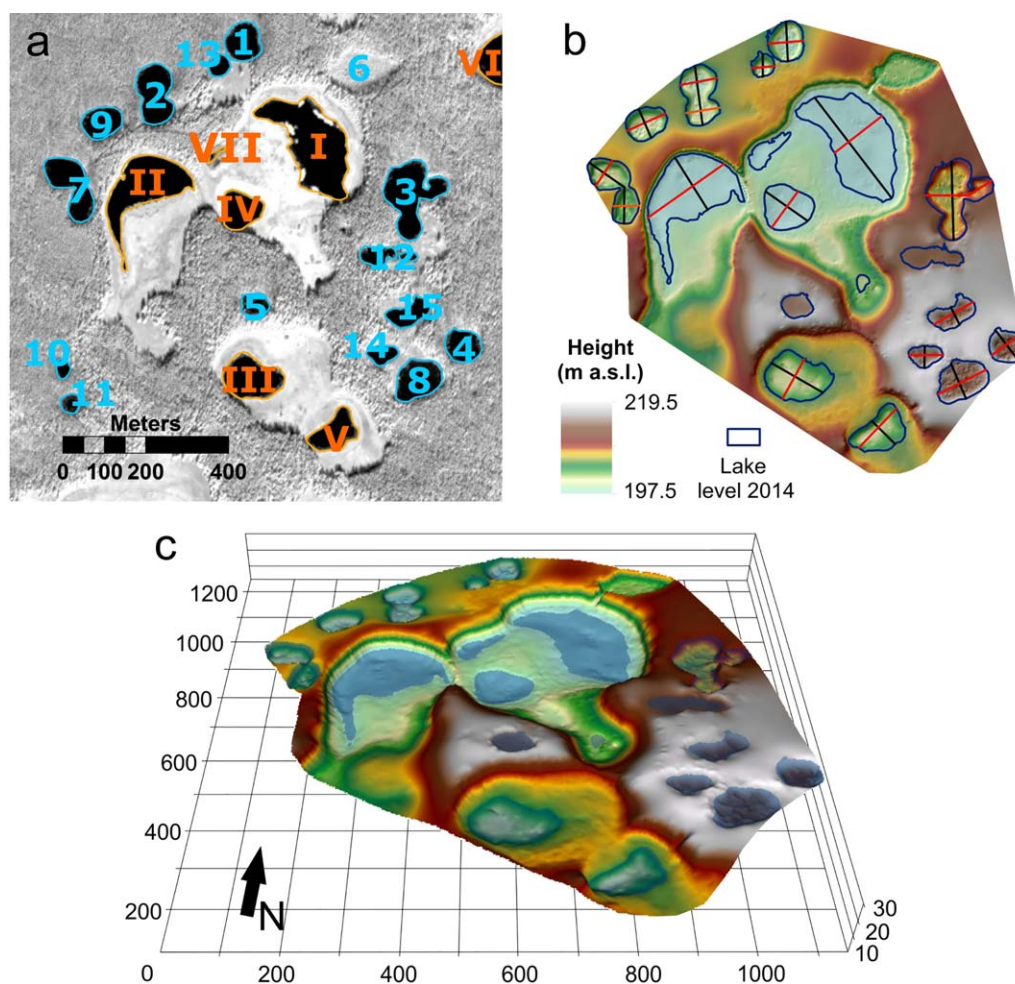


Figure 2. Lakes and topography of the Yukechi study site. (a) Pleiades satellite image close-up from September 2012 shows all studied lakes. All yedoma lakes are illustrated in blue and numbered by Arabic numerals. All alas lakes are illustrated in orange and numbered by Roman numerals (please see also supporting information Figure S1). (b) The Yukechi DEM. Ground resolution 0.5m, vertical accuracy (RMSE) 0.09 m, axis scale in meters and enlarged by 4X in Figure 2c. Lake levels in Figure 2b were measured in 2014. The black and red lines represent the topographic profiles shown in Figure 6; double lines in Lake 2 and 7 indicate different parts of coalesced lakes.

Fedorov and Konstantinov, 2003, 2008, 2009; Fedorov et al., 2014a]. In particular, small, young thermokarst lakes are ubiquitous on the yedoma uplands at the study site. Many of these yedoma lakes evidently developed anthropogenically (e.g., in former agricultural areas) [Fedorov et al., 2014a]. The Yukechi alas is one of three alas that represent our local main study site (Figure 2). The Yukechi alas is ~500 m in diameter and ~10 to 15 m deep. Two larger and one smaller lake exist within the alas; three more alas lakes occur in the neighboring alas. The very dry surface of the alas bottom is dominated by reddish halophytic grasses. The taiga forest covering the surrounding yedoma uplands ends at the upslope edges.

Before the soviet agricultural collectivization (until ~1930), the Yukechi area was dominated by traditional forms of agricultural management, predominantly related to cattle husbandry. After ~1930 until the 1960s, before the consolidation of collective farms, agricultural lands used for cereal crops were expanded around Yukechi. In particular, the Taiga forest on the yedoma uplands was used for cropland. Deforestation and stubbing were the basic method of clearing the land for cultivation. Since the 1960s all the local people have been moved to larger villages, and the small arable lands around the Yukechi alas are abandoned. At the beginning of the study by the Permafrost Institute Yakutsk in the early 1970s, arable land around Yukechi had already been withdrawn from agricultural use. Since then the development of the abandoned arable landscapes has happened without direct human impact.

3. Data and Methods

3.1. Mapping and Quantifying Local Lake-Area Changes

To quantify lake-area changes and to compare differences between alas and yedoma lakes as well as land-cover changes, all lakes within an area of ~1.4 km² at the Yukechi study site were mapped 10 times covering periods of 2–18 years between 1944 and 2012. In addition, field measurements of lake levels from 2014 were included in the time-series analyses. Lake boundaries were manually digitized within ArcGIS™ 10.1. from Russian historical black and white aerial photography as well as panchromatic and multispectral satellite imagery in high to very-high resolution with similar acquisition times from the end of summer (supporting information Table S1). All images were georectified to Universal Transverse Mercator (UTM) Zone 53, WGS84. Georeferencing was based on an orthorectified high-resolution multispectral Pleiades image (supporting information Table S1). Each image was rectified using at least 15 ground control points evenly distributed within the 1.4 km² study site, based on landmarks and features that were obviously present in both the rectified image and the Pleiades base-map image. The shore lines of lakes and ponds (in earlier stages of evolution) were mapped including only pixels that were clearly identifiable as water pixels. However, some shallow areas at alas-lake shores are covered by reed grass; this is known from field observations. These areas are mapped as part of the lake area because they could be unambiguously identified as such. In addition, area changes of the grasslands within alas basins and the cropland (i.e., meadows) on the yedoma uplands were mapped along the forest boundaries. In order to quantify rates of lake changes, the mean radius of each lake was then calculated following equation (1):

$$Lake\ radius\ (LR) = \sqrt{\frac{Lake\ area\ (LA)}{\pi}} \quad (1)$$

and the rate of lake radius change (RLRC) for a specific time (t) period was calculated in meters per year following equation (2):

$$RLRC = \frac{LR(t2) - LR(t1)}{Number\ of\ years} \quad (2)$$

Finally, for all types of land cover within the Yukechi study site, area and percent coverage were calculated for all time periods.

3.2. Field Work

Field work was conducted at the Yukechi study site in summer 2013 and 2014 to investigate alas- and yedoma-lake bathymetry, alas morphology, and surface characteristics. Detailed bathymetric data were collected for five alas lakes and eleven yedoma lakes in and around the Yukechi alas. A Garmin® GPSMAP® 421s echo sounder was used onboard a small rubber boat. Geographic location and water depth were recorded simultaneously and frequently as the boat moved across the lake along several transects. These

transects were arranged mainly from the lake center to the shore at frequent intervals to map the entire lake bottom. Local inaccuracies and gaps in depth measurements may have arisen from dense aquatic vegetation, sunken trees in active thermokarst lakes, and water-saturated bottom sediments.

An extensive geodetic field survey was conducted using a Topcon HiPer II dGPS (differential global positioning system) to study alas-basin and lake morphologies with a high-resolution digital elevation model (DEM). To ensure the highest vertical and horizontal accuracy, measurements were conducted only on treeless areas or open areas on yedoma uplands. The lake level was measured every two to four meters along the shoreline in July 2014. If the shoreline edge could not be identified accurately, the shoreline was defined as the level formerly measured at a clearly defined edge of the individual lake. Altogether, 9645 points were measured covering the Yukechi alas, the neighboring alases, and the general topography of the surrounding yedoma uplands. All points were stored in a coordinate-point database for interpolation to a raster data set.

3.3. Lake Volume and Subsidence Calculations

To calculate a hydrologically correct DEM of the Yukechi alas and its surroundings (Figure 2) we used the Topo-To-Raster tool within ArcGIS™ [Hutchinson, 1989]. All point measurements from the dGPS and bathymetrical surveys (in total 12,261 points) as well as the measured lake levels as contour lines were used as input data during processing. A grid-cell size of 0.5 m was chosen for the output DEM. Comparing modeled height values from the DEM to the original point database tested the vertical accuracy of the DEM. The root mean square error (RMSE) averaged 0.09 cm.

The DEM was used to extract lake-basin geomorphometry and volumes as well as to estimate bottom subsidence below yedoma lakes. For estimating subsidence rates, it was difficult to determine the original base height of the ground level before the thermokarst process began because the Abalakh terrace slopes to the northwest (Figure 2). Therefore, the 2014 measured lake levels were used as base height for subsidence calculations, because we know that the young thaw lakes on the Yedoma uplands are characterized by a relatively stable water regime [Soloviev, 1961; Fedorov et al., 2014a] and we simply assumed that the mean depth of the lake is related to the thawed ground-ice and hence corresponds to the amount of subsidence. Since the measured mean lake depth probably overestimates the real mean lake depth because of local inaccuracies and gaps in depth measurements, in particular in the shallow lake shore areas (see above), the calculated mean lake depths were used for subsidence estimations.

The calculated mean lake depth was determined using the dimension of each specific lake basin as extracted from the DEM and simple geometrical calculations of bottom radius, top radius, and volume of an upside-down truncated cone solved for height [Ulrich et al., 2010]; this was chosen to be the best geomorphological representation for the yedoma lakes at the Yukechi study site. For calculating the bottom radius of a lake it was estimated that the bottom area of a lake is nearly half the measured lake-water area, if one imagines the lake morphology as an upside-down truncated cone. Comparisons of the GIS-based calculated mean lake depth and the bathymetrically measured mean lake depth show good correlation. Yearly subsidence rates were deduced by dividing lake depth by the lake ages derived from the remote-sensing data (Table 1).

3.4. Climatological Data and Statistical Analyses

For identifying the climatological driving factors of yedoma- and alas-lake changes we used time series of air and ground temperature as well as precipitation from 1930 to 2014. Monthly air temperature and precipitation data were acquired from the Yakutsk meteorological station [NOAA/NCDC, 2016]. Monthly ground temperature data from 160 cm and 320 cm depths were used and averaged from four meteorological stations located within a radius of 50–100 km (Yakutsk, Pokrovsk, Churapcha) and 200 km (Okhotsk-Perevoz) from the Yukechi study site. In order to estimate annual lake-water balance we calculated potential evaporation (E_{pot}). Because evaporation calculation is always challenging and to reduce E_{pot} calculation uncertainties, we finally used the mean of two independent time series calculated using two different methods. First, the Blaney-Criddle method was applied according to Jones et al. [2011]. Second, annual E_{pot} was calculated by the Coupled Hydrological and Biogeochemical Model (CHANGE) developed by Park et al. [2011]. For details on E_{pot} calculation by both methods please see supporting information Text S1.

In order to statistically distinguish between long-term seasonal and annual influences on lake-area changes, air and soil temperatures and precipitation data were computed to different statistical environmental

variables representing hydrological year (October–September), winter (October–April), and summer (May–September) conditions. E_{pot} was computed to only one variable representing the entire hydrological year, assuming that evaporation in the preceding winter has only marginal influence on lake size. In a first step, a correlation analysis was performed on the long-term climate data to assess the relationships among all environmental variables over time. The *Pearson* correlation coefficient was calculated for a linear regression model connecting each environmental variable with TIME as well as for all possible combinations of two variables. Furthermore, to assess the relationship of lake sizes with TIME and possible similarities between the behavior of environmental parameters and lake sizes, a partial time series was derived from the all parameters, containing only years for which observations of lake sizes are available. Again, the *Pearson* correlation coefficient was calculated for linear regression models connecting lake sizes and TIME as well as for all combinations of lake sizes with environmental parameters. Derived coefficients were tested for statistical significance using an F-test and significance was assigned to the 95% confidence level.

In a second step, multiple linear regression models connecting the relationship of a set of environmental parameters to the changes in lake sizes were identified using *Pearson* correlation coefficients. Statistical significance of the models was tested using an F-test for the correlation coefficient and T-tests for the partial correlation coefficients for each parameter included in the model. Models are considered statistically significant if both the F-test and all T-tests yield significance at the 95% confidence level. The regression coefficients were standardized in the final models to allow comparability among the different environmental parameters. The partial time series was used in this approach, based on the assumption that the main influences of environmental parameters on lake sizes originated in the year previous to the lake-size measurement. This basic assumption is necessary due to the temporally sparse availability of lake-size measurements.

3.5. Mapping and Quantifying the Regional Lake Inventory

For analyzing the regional lake inventory we used a mosaic of Landsat 8 multispectral data. Three images, processed to Level 1T (standard terrain and radiometric correction), were obtained from the US Geological Survey (USGS) data archive. Two images (WRS Path/Row: 120/16 and 120/17) represent surface conditions on 26 July 2013. The third image (WRS Path/Row: 122/16) is dated to 24 July 2013. All three images were calibrated to top-of-atmosphere (TOA) reflectance using scene-specific metadata after *Chander et al.* [2009], projected to UTM Zone 53 North using the WGS84 ellipsoid with a spatial resolution of 30 m, and mosaicked to a large image using color balancing to match the statistics and to balance the data range between the different images. Finally, a spatial subset was extracted representing the study site of interest east of the Lena River (Figure 1a).

For automatic extraction of all water bodies we tested different approaches and compared the results qualitatively, in particular at our key sites, based on field knowledge, and in comparison to a high-resolution Pleiades satellite image. Because many small thermokarst lakes and ponds exist close together in the study region beside shallow alas lakes and flooded areas, the approaches were tested against lake separability, detection of small lakes with sizes down to one Landsat pixel (0.09 ha), and to minimize the mixed-pixel problem [*Muster et al.*, 2013] (supporting information Figure S2). Finally, we decided to extract the water bodies using the modified normalized water index (MNDWI) by *Xu* [2006]. The MNDWI was expressed following equation (3):

$$MNDWI = \frac{GREEN - SWIR}{GREEN + SWIR} \quad (3)$$

where GREEN is band 3 and SWIR is the shortwave infrared band 6 of Landsat 8 data. Using the ratio of green and SWIR reflectance from different land-cover types, the MNDWI enhances open-water bodies while strongly suppressing and removing noise from soil, vegetation, and developed land [*Xu*, 2006]. The application of the MNDWI results in a high-contrast image with pixel values between -0.69 and 1.0 . A threshold value of -0.05 was then applied to extract all water bodies because this provided the best balance between the abovementioned lake detection requirements (supporting information Figure S2b). The resulting data set was converted into vector polygons for subsequent processing and analyses in ArcGIS™ 10.1. After that, oxbow lakes and backwater pools on the Lena floodplains were excluded. Therefore, we used a clipping mask and defined its northern and western border by the 20 m a.r.l. contour extracted from a DEM. The clipping mask covers an area of 16,953 km². Within this area, all water pixels related to cloud shadows, drainage

channels, and small rivers and streams were manually removed. As a last step, a 10m buffer was used to merge a single pixel to the associated lake. The water pixels outside the buffer were considered to be stand-alone lakes. Finally, the areas of all remaining lakes were analyzed for the different geomorphological terraces (Figure 1b).

4. Results

4.1. Lake Area and Landscape Change at the Yukechi Study Site

Lake area changes and growth rates were investigated for 7 alas lakes and 15 yedoma lakes in total between 1944 and 2014 (Figure 3 and Table 1). While all the yedoma lakes are rather young (27 to ~74 years old) and were still developing during the observation period, the residual alas lakes probably existed long before and their number has not changed. However, the area covered by alas lakes has frequently changed since 1944. In 2014, the mapped alas lakes covered an area of 102,556 m², which is 7.2% of the study area (~1.4 km²); this is the largest amount covered by these lakes during the observation period. In 1944, the area covered by alas lakes was 4 times smaller (28,074 m², 2.0% of the study area), which is the smallest amount covered in the studied time period (Figure 4). Between 1944 and 1965 the alas-lake area remained more or less the same. In the two years from 1965 to 1967 the lake area more than doubled, and by 1971 it had increased to 78,424 m² (~5.5% of the study area). From 1971 to 1992 the total alas-lake area decreased to only 46,710 m² (3.3% of study area). The lake area increased dramatically from 1992 to 2010 and from 2012 to 2014 with a slightly slower rate between 2010 and 2012. The described changes in the alas-lake area are also clearly reflected in the averaged lake-radius changes of all alas lakes for the individual time periods as illustrated by the box-whisker plots in Figure 5. The mean RLRC of all the averaged values for all alas lakes over the whole observation period equals 1.6 ± 3.0 m/yr. Its high standard deviation represents the comparable high fluctuations and hydrological variability of the alas-lake area during the 70 years, with years of increasing and years of decreasing total alas-lake area. This becomes obvious when the individual growth rates of the 7 alas lakes are examined (see Table 1). The largest alas lakes within the Yukechi alas (Lake I and Lake II) exhibit the largest RLRCs and the highest lake-area fluctuations, with maximum increasing RLRC of 13.9 m/yr (Lake II) and 11.8 m/yr (Lake I) from 1965 to 1967 and maximum decreasing RLRC of -4.6 m/yr (Lake I) and -2.0 m/yr (Lake II) during the 1987–1992 period. Exceptions and outliers in the statistics are Lake VII, which is a very shallow pond that exhibits extreme fluctuations in water level and completely dried out during 1967, 1980, and 2014, and Lake VI, which is a small alas lake located to the northeast in another alas system that completely dried out in 1965 and 1987 (see Figures 3 and 5).

The area change of the yedoma lakes during the observation period shows a completely different picture. With the exception of Lake 1, Lake 4, and the northern part of Lake 2, all yedoma lakes developed in abandoned croplands and forest-free open grasslands around the Yukechi alas (Figure 3; see also section 2). The total yedoma-lake area increased constantly between 1944 and 2014 and almost all yedoma lakes are always expanding as shown by the always-positive mean growth rates for the individual time periods in Figure 5. None of the observed lakes shows clear signs of oriented migration. Instead, all yedoma lakes are expanding in every direction equally. The total lake area expanded by 40 times during the 70 year observation period. In summer 2014, the 14 measured yedoma lakes covered an area of 87,239 m², which equals 6.1% of the Yukechi study area. In 1944, only four lakes existed as very small ponds; two lakes (Lake 3 and Lake 4) were just beginning to grow. The two other lakes (Lake 1 and Lake 2) had probably started to grow a few years before. Altogether, in 1944 the yedoma lakes covered an area of only 2194 m², < 0.2% of the study area (Figure 4). By 1967, the area had increased to 16,784 m² (~1.2% of the study area) and three additional ponds existed. The highest yedoma-lake growth rates occurred between 1965 and 1967 (Figure 5). After 1971, growth rates were smaller and some lakes even decreased in area, particularly between 1980 and 1987; however, the number of existing and newly developed lakes increased from 9 to 15 during the same time period. While the alas-lake area shows high variability and kept decreasing until 1992 as described above, the yedoma-lake area increased further during the 1987–1992 period to 57,216 m² (~4.0% of the study area, Figure 4). The time between 1992 and 2010 is characterized by another 1.1% increase of the yedoma-lake area. Even though the mean growth rate is rather small as calculated for the 18 year time span (Figure 5), all yedoma lakes were growing during that time while some lakes decreased during other time periods. In particular, the area of the youngest yedoma lakes southwest and southeast of the

Table 1. Geomorphometric Characteristics, Mean Subsidence Rates, and Mean Growth Rates for All Studied Alas and Yedoma Lakes at the Yukechi Study Site^a

ID	Radius (m)	Surface Area (ha)	Volume ^b (m ³)	Lake Level ^d (m a.s.l.)	Mean Depth ^e (calc., m)	Mean Depth (meas., m)	Max. Depth (meas., m)	Age ^e (years)	Subsidence ^f (cm/yr)	Mean RLRC (m/yr)
Alas Lakes										
I	106.4	3.6	35,652	200.2	1.4	1.8	2.8	N/A	N/A	1.6 ± 4.1
II	96.7	2.9	38,621	200.9	1.8	2.2	3.3	N/A	N/A	2.1 ± 4.6
III	67.0	1.4	19,772	205.8	1.9	1.9	2.6	N/A	N/A	1.3 ± 2.9
IV	57.4	1.0	13,152	201.1	1.7	1.9	2.5	N/A	N/A	1.1 ± 2.2
V	55.0	1.0	14,696	206.2	2.1	2.3	3.6	N/A	N/A	1.0 ± 1.9
VI ^g	43.0	0.6	N/A	N/A	N/A	N/A	N/A	N/A	N/A	3.2 ± 7.9
VII	34.3	0.4	N/A	200.9	N/A	N/A	N/A	N/A	N/A	0.8 ± 4.1
Mean	65.7	1.6	24,379	202.5	1.8	2.1	3.0	N/A	N/A	1.6 ± 3.0
Yedoma Lakes										
1	46.5	0.7	17,296	205.8	3.5	4.0	5.3	74	4.7	1.1 ± 2.0
2	57.5	1.0	24,108	205.6	3.2	3.4	5.4	74	4.3	0.8 ± 1.7
3	74.5	1.7	44,942	211.6	3.5	3.6	5.6	70	5.0	0.9 ± 0.6
4	42.5	0.6	14,245	217.9	3.4	3.7	5.0	70	4.9	0.5 ± 1.2
5	32.7	0.3	2150	215.5	N/A	N/A	N/A	49	N/A	1.1 ± 1.9
6 ^g	52.3	0.9	N/A	N/A	N/A	N/A	N/A	49 (drained 2007)	N/A	1.3 ± 2.7
7	59.0	1.1	24,587	207.5	3.1	3.3	4.7	47	6.5	2.0 ± 2.2
8	55.2	1.0	18,801	217.0	2.7	2.5	4.0	43	6.2	1.6 ± 2.6
9	44.9	0.6	13,735	206.3	2.9	3.4	5.0	34	8.7	0.9 ± 1.3
10 ^g	20.1	0.1	N/A	N/A	N/A	N/A	N/A	27	N/A	0.7 ± 0.2
11 ^g	23.5	0.2	N/A	N/A	N/A	N/A	N/A	27	N/A	0.9 ± 0.9
12	42.1	0.6	1147	214.1	N/A	N/A	N/A	27	N/A	1.8 ± 1.1
13	28.1	0.3	4023	206.1	2.2	3.4	4.9	27	8.2	1.1 ± 1.1
14	32.0	0.3	4718	216.7	2.0	2.3	3.2	27	7.4	1.2 ± 1.3
15	41.6	0.5	6550	216.2	1.6	2.2	3.0	27	6.1	2.0 ± 1.2
Mean	46.4	0.7	14,692	211.7	2.8	3.2	4.6	47.4	6.2 ± 1.4	1.2 ± 1.0

^aMeans of subsidence and growth rates are given with standard deviation. Alas lakes are numbered according to their area. Yedoma lakes are numbered according to their age. For each lake location see also Figure 2 and 3.

^bCalculated from DEM.

^cMeasured in 2014.

^dCalculated from DEM.

^eLake age is estimated according to the first appearance in the satellite data (see Figure 3).

^fCalculation based on the calculated mean lake depth and age.

^gLake characteristics measured in 2012 for Lake VI, Lake 10, and Lake 1, and in 1992 for Lake 6.

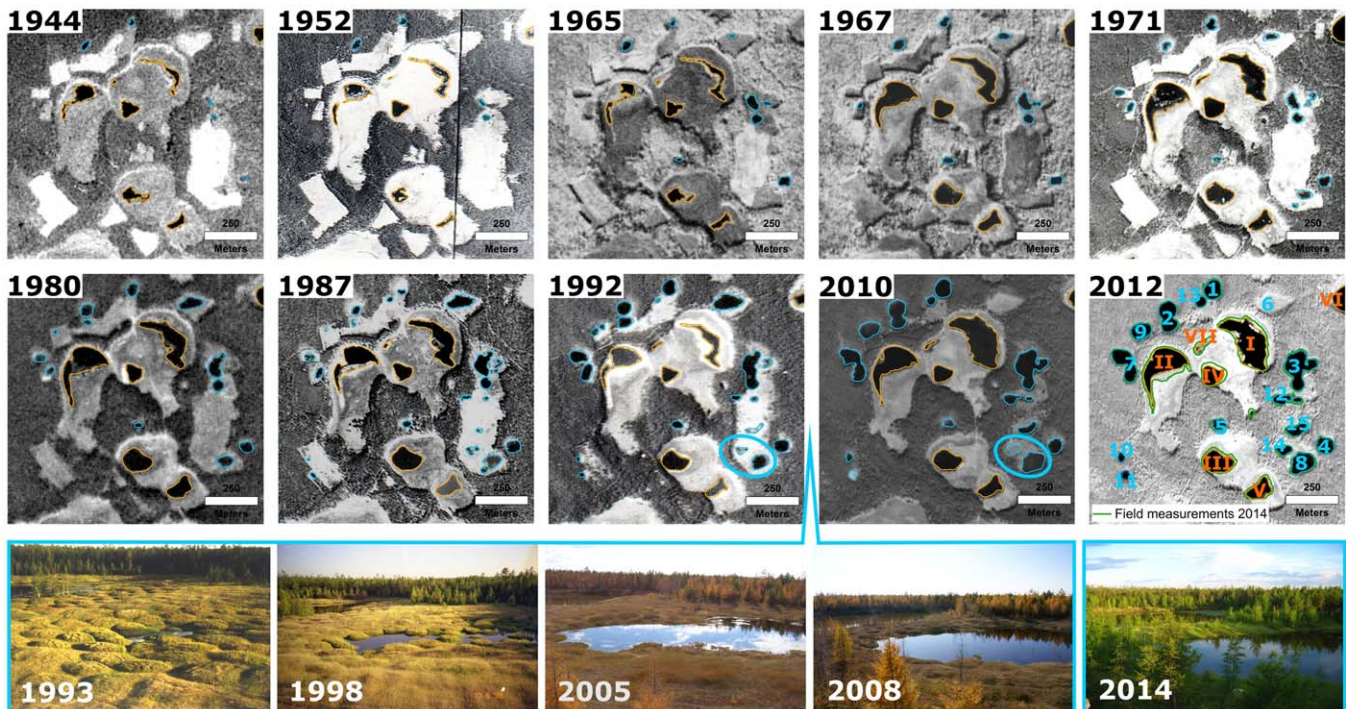


Figure 3. Aerial and satellite image time series of yedoma- and alas-lake changes and growth at the Yukechi study site. The bright areas around the Yukechi alas seen in the 1944 and 1952 aerial images mark arable land that has been abandoned completely since the 1960s. The blue ellipses in the 1992 and 2010 images mark the view from the northwest within photographs below. The photographic time line illustrates the rapid evolution of Lake 14 on the yedoma uplands.

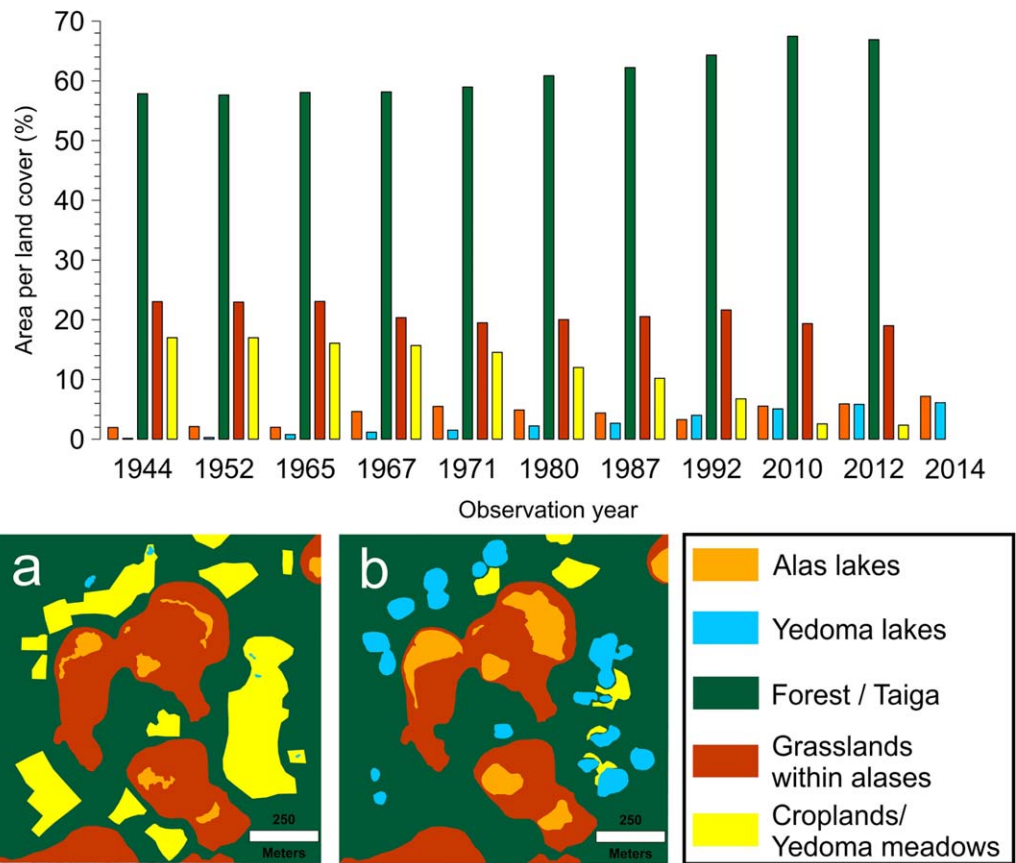


Figure 4. Land cover compared to lake changes at the Yukechi study site. The diagram shows the mapped change in areal percentage per land cover type over the whole time period. For the year 2014 only the lake coverages are shown. The maps show examples of land-cover distribution within the ~1.4 km² study sites for (a) 1944 and (b) 2012.

study area increased quickly. The largest yedoma lakes in Yukechi (Lake 3, Lake 7, and Lake 2) were finally formed during that time by the coalescence of 2 or 3 previously existing smaller lakes. Only Lake 6 drained to the Yukechi alas in spring 2007 after exceptionally high winter precipitation [Iijima *et al.*, 2010], which explains the negative outlier in the statistics (Figure 5). This event also contributed decisively to the area increase of Lake I within the Yukechi alas.

The constant increase and smaller fluctuations of the Yedoma-lake area is also represented by the mean RLRC for all yedoma lakes over the whole observation period, which equals 1.2 ± 1.0 m/yr. Individual growth rates for the 15 yedoma lakes are similar to the RLRCs of the alas lakes but the fluctuations (i.e., standard deviations) are smaller as shown by the smaller standard deviations in Table 1. Additionally, none of the yedoma lakes dried out after 1952 (Figure 3). Generally, lakes which started to grow after 1967 have higher growth rates and fewer fluctuations than lakes that existed before 1967. The highest mean RLRCs can be observed for Lake 15 (2.0 ± 1.2 m/yr over 27 years), Lake 7 (2.0 ± 2.2 m/yr over 47 years), and Lake 12 (1.8 ± 1.1 m/yr over 27 years). The lowest mean RLRCs are exhibited by Lake 4 (0.5 ± 1.2 m/yr over 70 years), Lake 10 (0.7 ± 0.2 m/yr over 27 years), and Lake 2 (0.8 ± 1.7 m/yr over ~74 years).

Finally, changes and growth of alas and yedoma lakes accompany land cover changes at the Yukechi study site (Figure 4). The grassland and meadow area within the alas system, which is used by the local population for hay harvesting, increases and decreases with the fluctuations of the alas lakes. The area on the Yedoma uplands covered by meadows and former croplands has steadily decreased from 17% in 1944 to 2.3% in 2014 due to the constant expansion of the yedoma lakes and the quick natural reforestation by birches and pines, in particular after the 1980s. During the whole observation period, no remarkable loss of forest vegetation due to lake expansion was identifiable, although yedoma lake shores north of the Yukechi alas are characterized by many tilted (“drunken”) and dead trees surrounding the lakes.

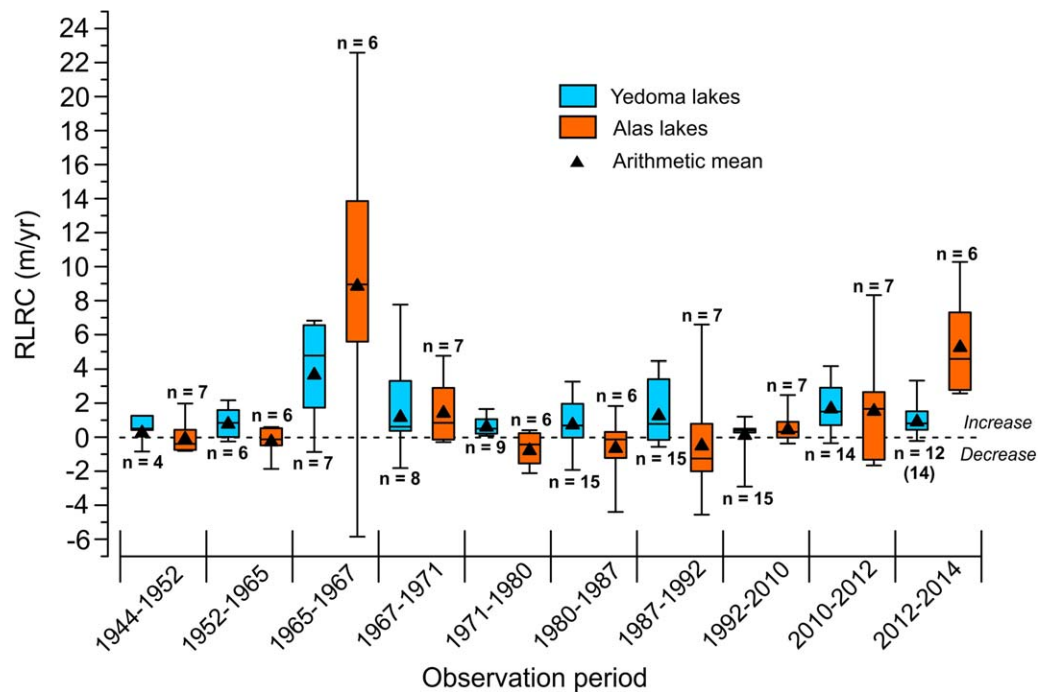


Figure 5. Box-Whisker plots illustrating the rates of yedoma- and alas-lake radius changes (RLRC) for different time periods. The mean RLRCs during the individual time periods are plotted additionally. The boxes are defined by the lower and upper quartiles. The line in the center represents the median and the whiskers at the end of each box indicate minimum and maximum outliers.

4.2. Lake Geomorphometry and Subsidence

The Yukechi DEM (Figure 2) and the topographic profiles (Figure 6) show the differences between yedoma lakes and alas lakes in bathymetry and basin morphometry. Example photos of alas and yedoma lakes are shown in supporting information Figure S1. The alas lakes have maximum measured depths ranging from 2.5 to 3.6 m. Their mean depths vary from 1.8 to 2.3 m (Table 1). The largest alas lake (I) exhibits the shallowest mean water depth, while the smallest measured alas lake (V) is characterized by the deepest water. Lake VII and Lake VI were not measured bathymetrically during summer 2014, because the first was very shallow with a maximum depth of ~ 0.6 m and the second is not part of the Yukechi alas system. The alas lakes are quite different in their basin morphometry. As shown in Figure 3, the water depths of the largest alas lakes (Lake I and Lake II) and also Lake V increase slightly from the alas-basin centers in the alas slope direction (Figure 2). Undercut features and bluff erosion mark the sites where the lakes have direct contact with the alas-basin slopes. With the exception of these areas, no bank erosion was observed around the lakes within the Yukechi alas. Lake shores are rather gently sloping and covered by reed grasses. Lake III and Lake IV show a rather bowl-shaped basin morphology suggesting that uniform thaw processes occurred during formation. The alas surrounding Lake III is also approximately circular (Figure 2 and supporting information Figure S1).

The yedoma lakes are clearly deeper than the alas lakes and have a rather uniform basin morphometry (Figure 6). Almost all yedoma lakes are characterized by a bowl-shaped basin morphology with steeply dipping shores and water depth that increases rapidly within 10–20 m of the lake shore until the maximum water depth is reached (Figure 2). Lake bottoms are generally flat and sometimes slope slightly from south to north, but many of the yedoma lake bottoms are hilly or hummocky. Maximum measured depths range from 3.0 to 5.6 m, while mean depths vary from 2.2 to 4.0 m. In general, the water depth of the yedoma lakes increases with age (Table 1). Individual subsidence rates, however, decrease with age. The highest subsidence rates were calculated for Lake 9 (34 years) at 8.7 cm/yr and Lake 13 (27 years) at 8.2 cm/yr. The lowest rates are shown by Lake 1 and Lake 2 (both ~ 74 years) at 4.7 and 4.3 cm/yr, respectively. The mean annual lake-bottom subsidence for all yedoma lakes at the Yukechi study site is 6.2 ± 1.4 cm/yr.

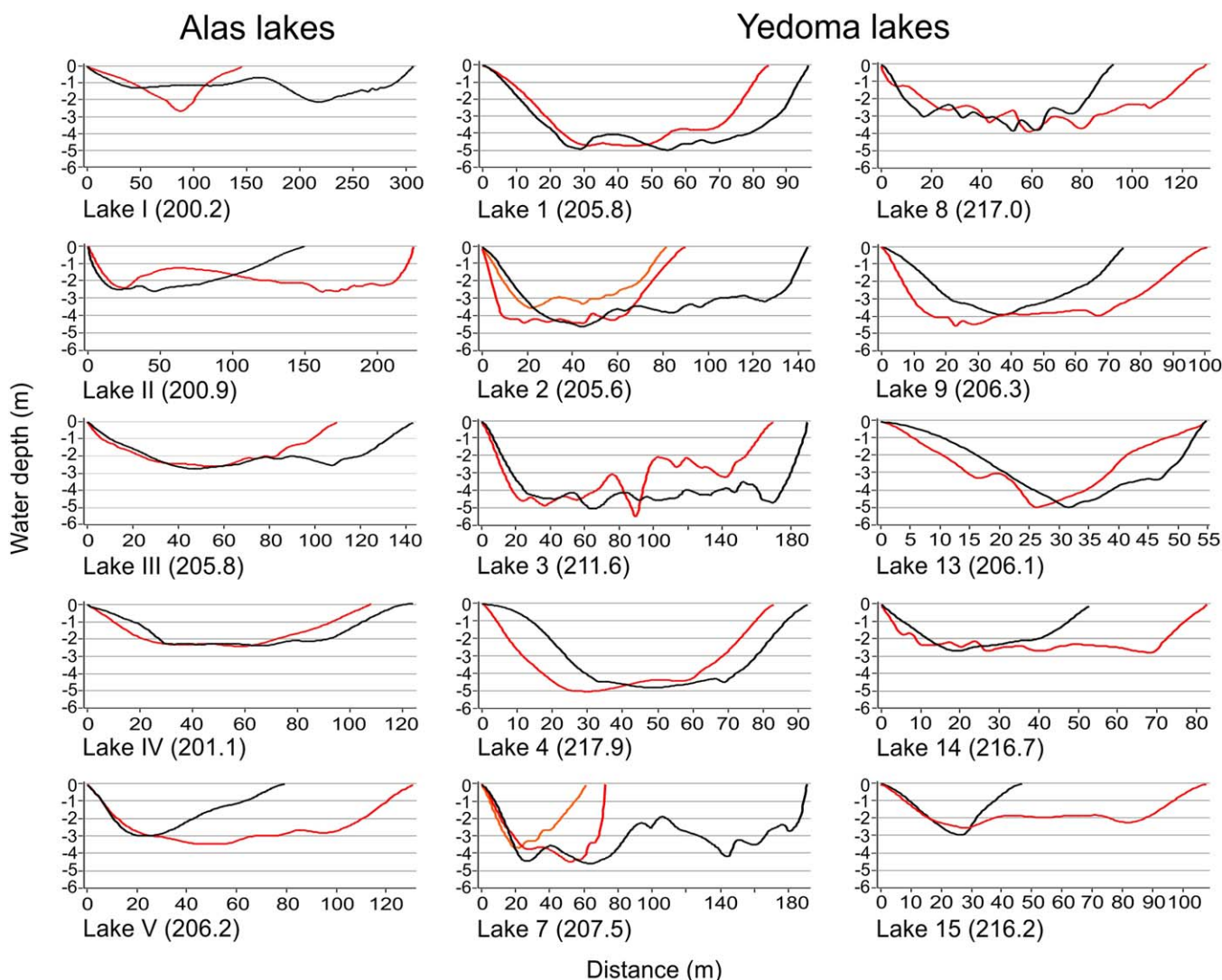


Figure 6. Lake bathymetry extracted from the Yukechi DEM (see Figure 2b) for all measured alas and yedoma lakes. Profiles always run below the 2014 water level (given individually in parentheses) from north to south (black lines) and west to east (red lines; additional orange lines in coalesced lakes 2 and 7). Note the differences in scales of the y axes.

4.3. Statistical Relationships of Climate Parameters and Lake Change at Yukechi

Climate data and permafrost temperatures from Yakutsk and other meteorological stations were analyzed to study seasonal and annual climatological variations within the different observation periods and the differences between alas- and yedoma-lake changes (Figure 7). All time series exhibited strong subdecadal variability, with generally increasing trends over the whole time period. The strongest increasing trends are shown by the mean winter (MWAT) and mean annual air temperature (MAAT) as well as the mean winter and annual ground temperatures at 160 cm depth. Air temperatures oscillate fairly equally until 1990. After 1990, there is a strong shift in the data; the mean summer air temperature (MSAT), MWAT, and MAAT remain almost constantly above their long-term means. The strongest statistically significant trend of $\sim 0.5^{\circ}\text{C}$ per decade is shown by the MWAT. The mean annual ground temperatures at the 160 cm ($\text{MAGT}_{-1.6\text{m}}$) and 320 cm ($\text{MAGT}_{-3.2\text{m}}$) depths show a tendency to increase by $0.03^{\circ}\text{C}/\text{yr}$ and $0.02^{\circ}\text{C}/\text{yr}$, respectively; that is the same as values reported already by others, e.g., Romanovsky *et al.* [2007]. We interpreted the variable mean summer ground temperature at the 160 cm depth ($\text{MSGT}_{-1.6\text{m}}$) as an indicator for variations in the active layer. In particular the $\text{MAGT}_{-1.6\text{m}}$ shows a strong increasing trend since the 1970s, with maximum annual values around 1970, 1980, 1990, 2000, and 2007. This trend is mainly determined by a strong increase of the $\text{MWGT}_{-1.6\text{m}}$ (Figure 7). While the $\text{MWGT}_{-1.6\text{m}}$ is increasing by $\sim 0.6^{\circ}\text{C}$ per decade, the $\text{MSGT}_{-1.6\text{m}}$ is decreasing slightly by $\sim 0.05^{\circ}\text{C}$ per decade. The precipitation data show high oscillations

during the whole time period but comparably low increasing trends. The increase of winter precipitation ($PREC_{Winter}$) is slightly higher than that of summer precipitation ($PREC_{Summer}$). $PREC_{Winter}$ was below the long-term mean until about 1950. Between 1952 and 1971, there was a strong oscillation; years of high values alternated with one to three years of lower values. After that time, the $PREC_{Winter}$ has oscillated more closely around the mean of 70 mm/yr, especially between 1972 and 1993, but there are repeated years of very high values; 1979/1980, 1988/1989, and 2006–2008. Because evaporation was calculated in the context of air temperatures, the value of E_{pot} parallels the MAAT. Concurrently, the annual water balance ($P-E_{pot}$) exhibits a slightly negative trend. However, both time series oscillate over the whole time period. In particular, the $P-E_{pot}$ time series reveal that years with drier conditions are always followed by more humid years, e.g., from 1948 to 1951, from 1986 to 1989, or between 2001 and 2007.

To provide a first quantitative estimate of relationships between environmental parameters and mean lake area, the *Pearson* correlations of all parameters among themselves and with the lake-area means (i.e., mean lake area in ha of all existing lakes at a certain time) were calculated for the partial time series that only contain years when lake areas were observed. Correlations between the environmental parameters and the lake-area changes are briefly described here. For more details on all parameter correlations please see supporting information Table S2 and Text S2. Overall, the statistics reveal that all environmental parameters have more influence on the yedoma-lake area than on the alas-lake area changes. The yedoma-lake area also shows a higher correlation with TIME ($r^2 = 0.97$) than does the alas-lake area ($r^2 = 0.80$), which probably confirms the fact that the yedoma-lake area increases throughout the covered time period, while the alas-

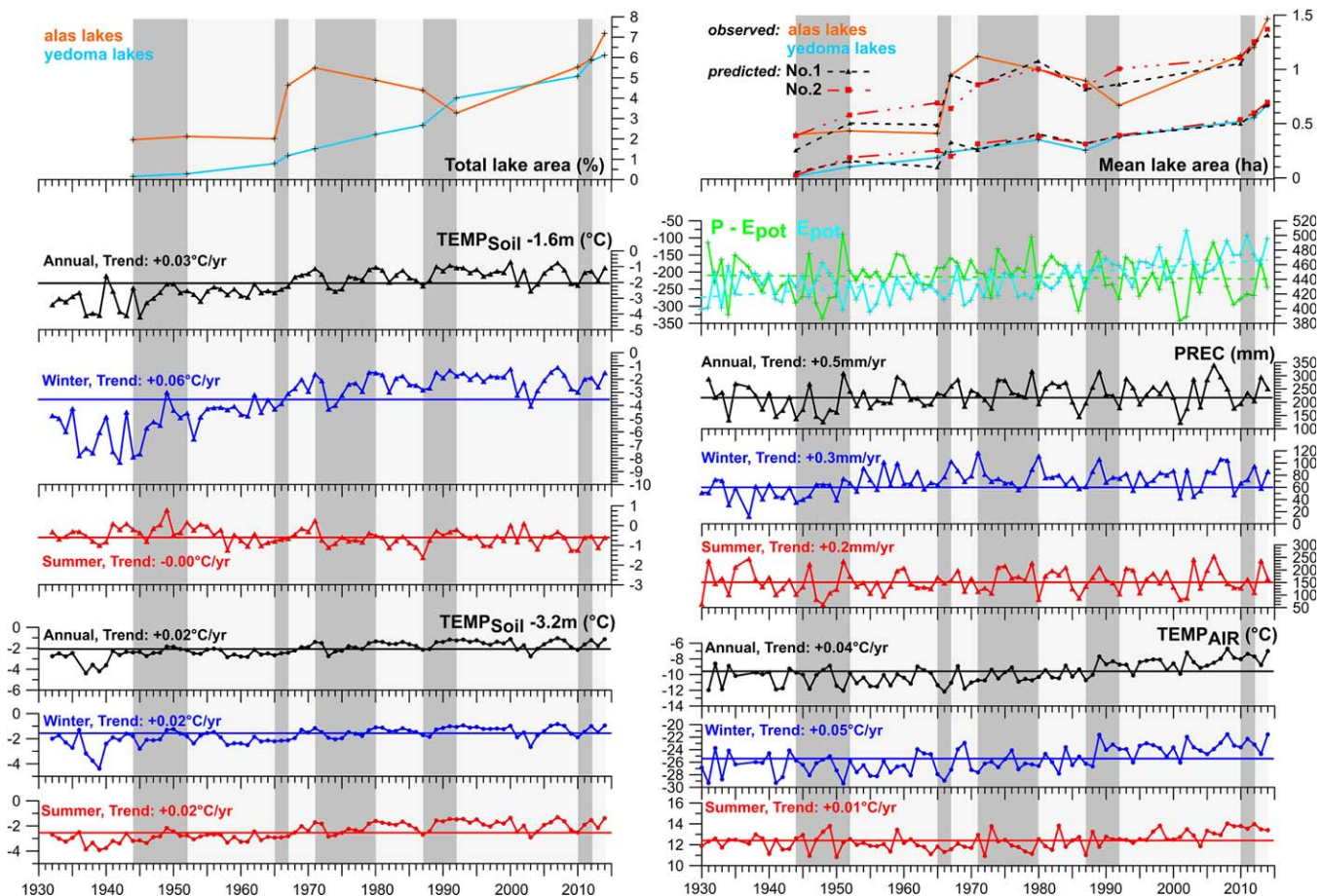


Figure 7. Climate data averaged over the hydrological year (October–September) from 1930 to 2014 for the studied region (please see text for details on acquisition and processing). For comparison, the total alas- and yedoma-lake area in percentage of study area (above, left side) as well as the mean lake area as observed and predicted by Model No.1 and No.2 (above, right side; see Table 2) are plotted for 11 times between 1944 and 2014 (Note: The mean lake area is calculated from the total lake area divided by the number of lakes existing during the certain time period). The studied time periods are highlighted by vertical grey bands (see also Figure 5). Solid lines indicate the mean of each environmental parameter over the covered time span.

lake area oscillates. The alas-lake area shows statistically significant, positive correlations with $MWGT_{-1.6m}$; $MWGT_{-1.6m}$ also correlates with TIME. Yedoma-lake sizes are significantly correlated with this parameter, but additionally with MAAT, MWAT, E_{potr} and $MSGT_{-3.2m}$ (supporting information Table S2). However, only $MSGT_{-3.2m}$ is not significantly correlated with TIME. Some noteworthy relationships are, however, not statistically significant, such as the negative correlation of the $MSGT_{-1.6m}$ with the areas of both kinds of lake, and the higher correlation of the $PREC_{winter}$ with the alas-lake area.

For a combination of different environmental parameters in statistical analyses and the prediction of their collective relevance to yedoma- and alas-lake area changes, multiple regression analyses were applied (Table 2). The multiple regression analyses, performed to connect various results and to elucidate their relationship to the environmental parameters, are presented and discussed below.

4.4. Regional Lake Distribution and Conditions

In total, 17,967 lakes larger than a Landsat pixel (0.09 ha) have been classified in the Lena Aldan interfluvial region mapping area (16,953 km²), covering an area of 958 km². This corresponds to an overall limnicity (land area covered by lakes) for the total study area of 5.7% (Figure 8). The average size of all lakes is 5.34 ha. The occurrence of numerous small lakes becomes obvious when all lakes are classified into seven different classes. Of all mapped water bodies, ~16,200 lakes are smaller than 10 ha; of these, 10,000 lakes are smaller than 1 ha, corresponding to about 25% of the total lake area. However, the largest proportion of the total lake area (~70%/~1700 lakes) is covered by middle-sized lakes (>10 – 500 ha). Only 7 lakes fall into the >500 – 1000 ha class and only one lake in the study area is larger than 1000 ha. Five of these lakes, including the largest lake of the whole study area (~1750 ha), belong to the lower Tyungyulyu terrace (65–100 m a.r.l.) and two of them to the lowest Bestyakh terrace (55–75 m a.r.l.).

The limnicity generally decreases from the lower terraces to the higher terraces. This difference with respect to elevation is reflected when lake density (number of lakes per 10,000 ha) is compared among the different terraces. The lake density on the lower terraces is more than twice as high as on the higher terraces (Figure 8). The differences between the terraces become more obvious when comparing the lake distribution in the various size classes. The middle and higher Abalakh, Magan, and Emilsk terraces are dominated by small lakes (<10ha) which account for ~40% of the lake area. If 10–25 ha class lakes are included, this corresponds to two-thirds of the total lake area on these terraces. In contrast, two-thirds of the Tyungyulyu and Bestyakh terrace lake areas are covered by lakes >25 ha. Many of these large lakes occur as residual lakes in large alases. This disparity is also expressed by comparing the mean lake sizes of all terraces (Figure 8). The largest percentage of area covered by lakes <1 ha (5.7%/N = 1743) was found for the Abalakh ice-complex terrace. A large proportion of these very small lakes are rather young and active thermokarst lakes located on the yedoma uplands, as we will describe in the next section. The largest number of the <1 ha class was found for the Tyungyulyu ice-complex terrace (N = 4978). However, this terrace has an area approximately twice the size of the Abalakh terrace.

5. Discussion

5.1. Differences in Yedoma- and Alas-Lake Morphology, Expansion, and Subsidence

The morphology of alas and yedoma lakes at the Yukechi site reflects their individual lake-basin evolution as well as local dynamics of thermokarst processes. The bathymetry of alas lakes suggests general surface stability within the alas basin. Vertical thawing below shallow lakes has almost ceased, either because alas basin bottoms have already reached the base of the ice-complex deposits, or because ice-depleted ice-complex residuals form an insulating layer that prevents further thaw processes [see *Morgenstern et al.*, 2011]. At the Yukechi site lateral but obviously very slow thaw processes are restricted to a few areas where the alas lakes have direct contact with the alas basin slopes. *Séjourné et al.* [2015] found large retrogressive thaw slumps along the banks of large thermokarst lakes and alases approximately 100 km north of Yukechi, where headwalls are retreating at rates of up to 3.16 m/yr. Generally, we can conclude that alas lakes are currently not expanding laterally due to thermokarst processes. Considerable bank retreat within the Yukechi alas and in its surroundings was not observed. Alas-lake area changes are instead highly variable and result from variations in the climatic and hydrological conditions. However, increasing lateral thaw degradation at the alas-basin slopes in the future could be the result of persistently high alas-lake levels due to increasing lateral heat fluxes from the lakes to the basin slopes and subsequent undercutting and oversteepening of the slopes [*Kokelj et al.*, 2009; *Grosse et al.*, 2013].

Depth, bathymetry, and growth rates of the yedoma lakes reveal the high thermokarst potential and surface instability on the yedoma uplands (Table 1 and Figure 6). The 15 studied yedoma lakes represent different stages of evolution, but all these lakes rapidly evolved after forest destruction within ice-rich permafrost deposits. The yedoma lakes exhibit a clear age-depth relationship ($R^2 = 0.74$); lake depth increases with lake age (supporting information Figure S3). However, there is an inverse, though small, relationship between lake age and expansion rate (i.e., RLRC; $R^2 = 0.32$) and, in particular, between age and subsidence rate ($R^2 = 0.35$); this suggests that younger and shallower lakes are growing faster than older and deeper lakes at the study site (supporting information Figure S3). However, two main points must be discussed here. First, our data suggest that time is an important factor as shown by the statistics described in section 4.3, and that thermokarst processes have accelerated, especially during the last two decades, as a consequence of increasing permafrost temperatures and winter precipitation [Iijima *et al.*, 2010, 2016]. Second, to understand growth rates of the yedoma lakes, we need to consider two different landscape types. All the lakes with higher growth rates evolved after 1967 in abandoned croplands and forest-free open grasslands, while especially the older yedoma lakes such as Lake 1, Lake 4, and the northern part of Lake 2, but also other lakes with lower expansion rates, such as Lake 10 and Lake 11, are currently in the process of being and/or have already been surrounded by forest (Figure 3, see also supporting information Figure S1). In some cropland areas, the fast overgrowth by pine forest has probably slowed the expansion of thermokarst lakes. The insulating effect of the forest cover hampers lake growth in comparison to growth in open grassland areas [Fedorov and Konstantinov, 2009; Lara *et al.*, 2016].

Calculated subsidence rates for the yedoma lakes (mean 6.2 ± 1.4 cm/yr) are cautious estimates averaged over the whole observation period and deduced from the 2014 lake level (Table 1). They are, however, in the same range as data from Fedorov *et al.* [2014a] for one lake at the Yukechi study site. Fedorov *et al.* [2014a] also found an acceleration of thermokarst activity during the last decades with increasing subsidence rates, up to 17.6 cm/yr, during 2004–2008. The mean RLRC of all yedoma lakes (1.2 m/yr) exceeds the expansion rates of thermokarst lakes from other continuous permafrost regions, which usually range from 0.3 to 0.8 m/yr [Grosse *et al.*, 2013, and references therein]. Exceptionally high RLRCs, between ~ 4 m/yr and ~ 7 m/yr, have been observed for individual Yukechi yedoma lakes for the time periods 1965–1971, 1987–1992, and 2010–2014, but some older lakes that existed before 1967 also show decreasing RLRCs of -1.5 to -1.9 m/yr during 1967–1971 and 1980–1987. This suggests that expansion rates and lake area changes can be variable from site to site in connection with certain preconditions such as cryolithology (i.e., permafrost properties, sediment type), reason for initiation, vegetation, and topography, as well as lake size and bluff height of surrounding lake margins [e.g., Jones *et al.*, 2011; Kessler *et al.*, 2012; Lara *et al.*, 2016].

The hummocky floors of some yedoma lakes resolved in the bathymetric profiles are particularly interesting (e.g., Lake 8, 34 years old, Figure 6). This lake-bottom relief is formed by thermokarst mounds or baydzherakhs and reveals the remnant polygonal network within the ice-complex cover, in particular the location of former polygon centers that existed before ice-wedge melting. With these features, the yedoma lakes can be classified as *Dyuyodya* representing thermokarst lakes in early stages of development [Soloviev, 1973]. Further deepening can be expected, because the ice complex is not yet completely thawed. Nearly flattened floors as seen in the profile of, e.g., Lake 1 (~ 74 years old) are formed when the ice complex is almost completely thawed and the vertical thaw process has ceased. The lake can now be classified as *Tympa* and represents a preliminary alas stage [Soloviev, 1973]. This highlights just how quickly thermokarst lakes and alas basins can evolve in CY. Bosikov [1998] has suggested that thermokarst could reach a mature and stable stage as alas within 100–200 years in CY. Brouchkov *et al.* [2004] contended that 200–300 years are required to completely thaw an ice complex.

5.2. Trends in, Drivers of, and Differences Between Thermokarst Lake Changes and Evolution

Obviously, the change in the area of alas and yedoma lakes over the observed time period of 70 years cannot be explained by one environmental parameter alone (supporting information Table S2). Consequently, linear multiple-regression analyses were applied to predict yedoma- and alas-lake area changes independently using a certain combination of environmental parameters. This analysis requires that the considered environmental parameters are not linear combinations of each other; one parameter may not be derivable using the other parameters. In order to ensure that this condition is met, certain combinations of environmental parameters were excluded from the analysis (e.g., $PREC_{Annual}$ was not used in combination with E_{pot} and $P-E_{pot}$ and/or $PREC_{Annual}$ was not used in combination with $PREC_{Winter}$ and $PREC_{Summer}$, etc.). Model No.1 included a combination of $PREC_{Winter}$, MWAT, and $MSGT_{-1.6m}$ that explained equally a high percentage

Table 2. Multiple Regression Models and Final Selection of Environmental Variables That Predict Yedoma-Lake and Alas-Lake Changes^a

No.	R ²	Sig.	PREC _{Summer}		PREC _{Winter}		MSAT		MWAT		MSGT _{-1.6m}		MSGT _{-3.2m}	
			B	Sig _{part}	B	Sig _{part}	B	Sig _{part}	B	Sig _{part}	B	Sig _{part}	B	Sig _{part}
<i>Yedoma-Lake Change</i>														
1	0.94	0.0001			0.621	<0.0005			0.793	<0.0001	-0.341	0.0098		
2	0.98	0.0001	0.317	0.007			0.449	0.001			-0.534	0.0002	0.753	0.0008
<i>Alas-Lake Change</i>														
1	0.86	0.0022			1.366	0.001			1.019	0.006	-0.648	0.044		
2	0.69	0.0906	0.311	0.513			0.513	0.333			-0.774	0.118	1.261	0.049

Values in bold indicates the correlation coefficients of our regression models and their significance as discussed in section 5.2.
^aR² Correlation coefficient of the models. B Correlation coefficient for the individual environmental parameter. Sig./Sig_{part} indicates statistical significance of the model results and the correlation coefficient at the 95%-confidence level.

of the total variance in both kinds of lakes (for yedoma lakes $r^2 = 0.94$, $p = 0.0001$; for alas lakes $r^2 = 0.86$, $p = 0.002$; see Table 2). The model predicts that yedoma- and alas-lake areas will increase after a preceding warm winter with high precipitation (i.e., snow cover) and lower MSGT_{-1.6m} in the following summer (Figure 7). The latter suggests that a shallower active-layer depth may lead to larger lake areas. This is not surprising because it indicates that less water may infiltrate into the soil after snow melt, but may instead enter the lakes by interflow and surface runoff, leading to larger lakes. This interrelationship was also discussed by *Chen et al.* [2014]. Model No.1 also suggests a negative relationship between snow cover and summer ground temperatures (i.e., active layer depth), which might be due to the timing of snow fall and disappearance [*Ling and Zhang, 2003*] or the cooling effect of higher soil moisture as a result of higher snow cover [*Zhang et al., 2005*]. Developing a model which can predict the differences between the yedoma- and alas-lake changes has proved more difficult. However, Model No.2 could be developed for predicting yedoma-lake changes by combining the parameters MSAT, MSGT_{-1.6m}, MSGT_{-3.2m}, and PREC_{Summer} ($r^2 = 0.98$, $p = 0.0001$), which do not predict the observed alas-lake changes (Table 2 and Figure 7). The model simply predicts that the area of yedoma lakes is also increasing as a result of higher precipitation and air temperatures as well as higher ground temperature at the 320 cm depth, but lower ground temperatures at the 160 cm depth during the preceding summer. This point becomes particularly obvious when we look at the time period between 1970 and 1992, during which the observed alas-lake area in Yukechi continuously decreased, while the yedoma-lake area continuously increased.

Our statistical analyses reveal that increased yedoma- and alas-lake areas were equally influenced by a combination of winter precipitation and winter temperature. Shallower active-layer depths in the following summer, moreover, lead to enhanced water supply to all lakes after snow melt because the water cannot infiltrate deeper into the soil. It should be noted here that the larger catchment areas of alas lakes result in a higher water supply. Increasing permafrost temperatures have a larger influence on yedoma-lake growth because the thawing of the surrounding ice-complex deposits provides a significant water supply [*Fedorov et al., 2014a*]. The annual thermal permafrost conditions seem to be mainly determined by the MWGT, however. Permafrost degradation and thus yedoma-lake growth are further intensified if the mean air temperatures are high over the summer and if the summer is characterized by higher precipitation. Evaporation is frequently suggested to be the main driving factor of thermokarst lake decrease, along with lake drainage [*Riordan et al., 2006; Labrecque et al., 2009; Chen et al., 2014*]; evaporation and the water balance ($P-E_{pot}$) tend to play a less significant role in the long-term trend of yedoma- and alas-lake changes at the Yukechi study site (Figure 7) even if $P-E_{pot}$ shows high correlation with precipitation (supporting information Table S2). Rather, evaporation seems to have an indirect influence, because the ground temperatures (in particular at the 320 cm depth) tend to increase as the soil dries due to increasing evaporation (see also supporting information Table S2 and Text S2). On the other hand, increasing ground temperatures in the upper permafrost as a result of high winter precipitation as reported by *Iijima et al.* [2010] are also comprehensively documented between 2004 and 2007 in the time series described here (Figure 7). Short-term decreasing growth rates of some older yedoma lakes during 1967–1971 and 1980–1987 could have resulted as well from a small increase in evaporation and consequently a decrease in water balance. In the case of alas lakes, it seems that the influence of evaporation is related to the lake-surface area [*Roach et al., 2011*]. This could be an additional factor explaining the higher lake-area fluctuations of Lake I and Lake II and their lowest mean water depths (Table 2).

Climatic and environmental conditions have strongly affected the growth rates of yedoma lakes during certain time periods, but they did not lead to remarkable reductions of their areas or their disappearance during the observation period. The rapid evolution of these lakes was initiated by the destruction of the forest cover and the resultant decrease of the insulating shielding layer [Shur *et al.*, 2005; Fedorov *et al.*, 2014a]. Once initiated, the thermokarst processes accelerated over time and were intensified by the climatic conditions, in particular during the last two decades. However, differences appear because of anthropogenic or natural forest cover destruction. The yedoma lakes that developed in abandoned arable land after 1967 have grown faster than the older lakes that were probably initiated by allegedly natural processes such as forest fire or insect attacks. Additionally, as the yedoma lakes are aging it seems that their changes become less influenced by local thaw processes and more by climate conditions.

Alas lakes increase and decrease in size due to a combination of certain climatic and environmental factors. Our ability to distinguish the main controlling factors and the differences in predicted and observed alas-lake changes, however, is hampered, probably due to larger catchment areas and subsurface hydrological conditions. Since winter-ice thickness in the study area is usually less than 100 cm under current weather conditions (see section 2) and the depths of all measured lakes clearly exceed winter-ice thickness (see Table 1), taliks very likely exist beneath all measured lakes [Aré, 1969; West and Plug, 2008]. Indeed, taliks have been proven below alas Lake IV and yedoma Lake 4 during drilling activities in spring 2015 by unfrozen sediments that reached at least ~ 20 m and ~ 12 m below the water surface, respectively. However, while the taliks below the yedoma lakes are very likely closed, the taliks below the Yukechi alas lakes seem to be partly open, because a talik that reaches ~ 7 m below the ground surface was also found below the central dry and slightly elevated part of the northeastern alas basin (see Figure 2c). A large talik below the Yukechi alas would lead to lateral ground-water flow and hydrological connections between alas lakes. This could have had an important influence on the alas-lake water balance [Yoshikawa and Hinzman, 2003]; this is not yet established for certain, but could be one additional explanation of why the environmental parameters have less influence on the alas lakes than on the yedoma lakes in the statistics (supporting information Table S2).

Cyclical alas-lake area changes in CY have often been reported and discussed in the Russian literature. These cycles are interpreted to be influenced mainly by cyclical changes in precipitation and resulting variability of the general area wetness [Soloviev, 1961; Bosikov, 1998; Desyatkin, 2004; Tarasenko, 2013]. According to Soloviev [1961], periods of maximum lake level repeat every 19–45 years, while Bosikov [1998] mentioned 150-to-180 year wetness cycles as the most prominent. Cyclical precipitation variations can also be easily recognized in our precipitation time series (Figure 7); years with low and high precipitation alternate about every 5–10 years. These variations are not recognizable in the alas-lake area changes at Yukechi, emphasizing that precipitation alone is not responsible for interannual alteration of alas lakes [Plug *et al.*, 2008; Tarasenko, 2013], even if the short-term lake-area changes over longer time periods seen in our satellite data investigations cannot be reconstructed. The largest total alas-lake areas recognizable within our study occurred in 1971 and 2014 (Figures 3 and 4). This would correspond to the data by Soloviev [1961] and a period of decreasing alas-lake levels would be an imminent consequence. However, the contemporary climatic and hydrological situations at the Yukechi study site rather suggest the continuation of wet conditions and high alas-lake levels.

Finally, climatic conditions in CY have changed, especially after the 1990s. Increasing soil temperatures and active-layer deepening were observed as a consequence of increasing precipitation (winter and summer) and result in regionally wetter conditions [Iijima *et al.*, 2016]. The considerable area increase of the studied yedoma and alas lakes after 1992 is certainly a consequence of climate change. Our statistical analysis was aimed, however, at detecting the long-term trends in lake-area changes and the influencing environmental factors during the last 70 years. Distinguishing between the time periods before versus after 1990 was not possible for statistical reasons but should be investigated for several important factors and changes in the environmental variables with which they are correlated. Furthermore, short-term changes such as the exceptionally strong lake-area changes in the 1965–1967 period cannot be completely explained by our statistical analysis. Even if this strong lake-area increase is very well predicted by our regression Model No.1, the environmental parameter changes combined in this model are not exceptionally high during that time (Figure 7). This clearly shows the complex nature of thermokarst lake-area changes; these changes are influenced by a combination of different climatic parameters as

well as by variations in permafrost conditions, vegetation, and anthropogenic influences [Grosse et al., 2013].

5.3. Peculiarities of the CY Lake Inventory

Distribution and size of all mapped lakes differ clearly on all five Lena terraces, reflecting different geocryological and hydrological conditions. Differences are especially obvious for the two ice-complex terraces (Figure 8). The higher, older, and more ice-rich Abalakh terrace is characterized by lower lake density and smaller lakes, while the younger and less ice-rich Tyungyulyu terrace is characterized by the highest lake density and large lakes. There is also a clear trend toward higher density of larger lakes in the northern part of the mapped area (Figure 1). The overall limnicity for the mapped area (5.7%) is generally lower than values reported from other thermokarst-affected regions in the Northern Hemisphere, which can exceed 40% [Grosse et al., 2013], but is similar to values for yedoma uplands in the Laptev Sea region [Grosse et al., 2008; Morgenstern et al., 2011] or peatlands in northeastern European Russia [Sjöberg et al., 2012]. Similar to other thermokarst-affected regions is the large number of the small lakes (<10ha) that are especially important for hydrological and biogeochemical cycles [Grosse et al., 2008, 2013]. Not all of the studied lakes are thermokarst lakes, but they show evidence of geomorphological processes in connection with permafrost dynamics [Soloviev, 1959, 1973; Pestryakova et al., 2012; Boike et al., 2016]. All Tyungyulyu and Abalakh terrace lakes evolved in connection with thermokarst processes. Many of the low Bestyakh terrace lakes are water-filled old erosive depressions probably created by water inflow from the surrounding sand deposits. The high Magan and Emilsk terrace lakes are usually located in old valleys and many of them are freshwater lakes [Soloviev, 1959].

All larger lakes (>25 ha) on the Tyungyulyu terrace are water bodies within large alas that formed from interconnected smaller lakes. These large alas lakes are prone to cyclical lake-level changes [Soloviev, 1961; Bosikov, 1998]. While the distribution of larger lakes on the Abalakh terrace is also associated with alas basins, these alas basins are significantly smaller than those on the Tyungyulyu terrace (see also Figure 1). Lakes >500 ha are completely absent on the Abalakh terrace, due to complex and diverse hydrological and geomorphological conditions on the different terraces [Soloviev, 1959]. The relief of the lower Tyungyulyu

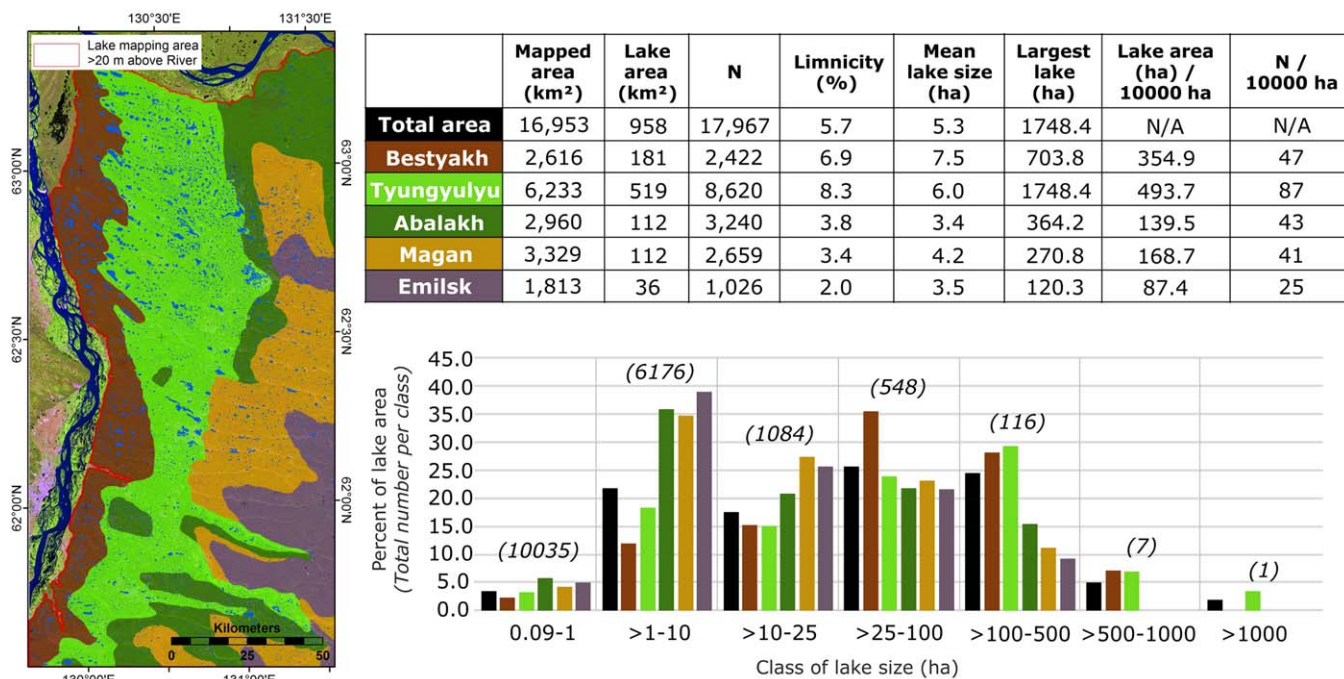


Figure 8. Lake inventory extracted from July 2013 Landsat 8 data for the different geomorphological terraces in the Lena-Aldan interfluvium region. The map shows the terraces within the mapping area in different colors. Area and extent of the terraces was compiled according to Soloviev [1959]. Elevation increases from WNW to ESE (see Figure 1b). The table summarizes lake statistics for the total studied area (black row) and the different terraces (rows colored according to map). Note in particular the differences between the Tyungyulyu (light green) and Abalakh (dark green) ice-complex terraces. The histogram below shows the percentage of total lake area (black bar) shared by various size classes compared to the different terraces (bars colored according to map).

terrace is almost flat. River and alas valleys are almost absent. This results in poor drainage on this terrace and regionally wetter conditions. The higher Abalakh terrace relief, however, is much more indented and the gently sloping yedoma uplands alternate with east-to-west-striking valleys (Figure 1). This improves drainage conditions in comparison to the Tyungyulyu terrace. Comparatively lower ice-complex thickness with lower ground-ice contents underlain by sandy deposits on the Tyungyulyu terrace [Soloviev, 1959] likely limited the vertical expansion but intensified the lateral expansion of thermokarst landforms [Ulrich *et al.*, 2010; Morgenstern *et al.*, 2011] and facilitated the large-scale coalescence of lakes and alas basins. The comparatively thicker but more spatially limited extent of the ice complex on the Abalakh terrace [Soloviev, 1959, 1973] likely intensified vertical thermokarst processes, which led to smaller but deeper alas basins and thermokarst lakes. The larger distribution of small- to medium-sized first-generation lakes on the yedoma uplands of the Abalakh terrace, as seen around the Yukechi study site, point to higher thermokarst activity here [Fedorov and Konstantinov, 2003; Grosse *et al.*, 2008].

Lake-change detection on a regional scale is necessary to study the changes of lakes within different size and type classes and on different geomorphological terraces. Preliminary lake-change studies by Ulrich *et al.* [2015] reveal that the area of all lakes in the Lena-Aldan interfluvial region has not increased considerably between 2007 and 2013, but the number of lakes is decreasing on the lower terraces, while increasing on the higher terraces during the same period of time. This would confirm that many of the small lakes (<10ha) on the high terraces are young, active thermokarst lakes on the yedoma uplands (referred to as yedoma lakes in the former sections) while many larger single lakes within alas basins on the lower terraces have likely coalesced from smaller lakes, reducing the number of lakes.

5.4. Possible Geo-Ecological and Socioeconomic Implications

According to the projected increase in precipitation (mainly winter precipitation) and air temperature in the boreal regions of CY [IPCC (Intergovernmental Panel on Climate Change), 2013; Bring *et al.*, 2016], permafrost temperatures and active-layer depth will continue to increase in the future. As a result, the thermokarst activity will remain at a high level and lakes will grow on the yedoma uplands, especially in areas subjected to progressive deforestation. In consequence, arable land will be abandoned due to surface subsidence and thermokarst-lake development. In addition, increasing permafrost degradation and thermokarst-lake development on ice-rich deposits could trigger growing forest damage due to persistent wet soil conditions and an oversaturated active layer [Iijima *et al.*, 2014; Lara *et al.*, 2016]. The current climate conditions also seem to favor persistently high alas-lake levels and wet conditions within alas basins. Indeed, wetter surface conditions within the CY alases than experienced during earlier times have been reported by the local inhabitants [Crate, 2011]. Wetter conditions will impact hay production within alases, will decrease inhabitants' access to the forest and other needed resources, and will threaten the stability of buildings [Crate, 2011]. However, increasing active-layer depth and evaporation together with decreasing precipitation could also lead to surface drying within the alases and less water supply to the lakes. Dry conditions within alas basins would be equally problematic, because alas lakes provide the only water supply for a large proportion of the Yakutian population [Desyatkin, 2004].

Regionally, geomorphological and hydrological conditions on the different terraces in the Lena-Aldan region must be considered. In previous eras of climate warming the better-drained surface of the Abalakh ice complex was suggested to be less affected by thermokarst processes than the more poorly drained surface of the Tyungyulyu terrace, which accumulated considerable amounts of surface and supra-permafrost water [Bosikov and Ivanov, 1978]. According to our regional and local studies, thermokarst activity seems to have increased on the higher terraces, however. The evolution of many young and small thermokarst (i.e., yedoma) lakes on the Abalakh terrace by thawing of icy deposits will increase the overall moisture regime on this terrace in the medium term. The high lake level on the Tyungyulyu terrace and the coalescence of smaller alas lakes to form lakes that fill alas basins almost completely will result in persistent wet conditions. Generally, this estimated trend, together with the results of previous studies [Tarasenko, 2013; Boike *et al.*, 2016], matches findings of increasing total lake area from other continuous permafrost regions [Smith *et al.*, 2005; Labrecque *et al.*, 2009]. However, the areas most vulnerable to permafrost degradation are those where the forest has been destroyed, naturally or anthropogenically. The estimated trend can thus be offset by local and regional variations in the vegetative land cover because permafrost stability is usually buffered below a forest canopy by a shielding layer that prevents underlying ice-rich deposits from thaw even under warm climate conditions [Shur *et al.*, 2005; Fedorov and Konstantinov, 2009].

As reported above, the young thermokarst lakes on Yukechi yedoma uplands expanded by 40 times during the 70 years of observation, during which huge amounts of ice- and organic-rich permafrost rapidly thawed. *Morgenstern et al.* [2011] discussed the differing thermokarst potential of lakes developing on yedoma uplands and lakes in existing thermokarst basins in the Lena Delta. They assume that lakes on yedoma uplands have stronger transformative impacts on permafrost landscapes and also on the mobilization of carbon stored in yedoma deposits than lakes existing within thermokarst basins, where further thermokarst potential is restricted because the underlying ice-depleted sediments have already been thawed and reworked. *Walter et al.* [2007] discussed the hypothesis that large atmospheric methane concentrations could originate from thaw processes of thermokarst lakes on yedoma deposits because these never-thawed deposits contain much more carbon than already-thawed deposits below drained thaw-lake basins. *Desyatkin et al.* [2009] could, moreover, show the differing potential of methane emissions from different stages of thermokarst (lake) formations in CY, and that young thermokarst formations on yedoma uplands have higher methane emissions from pond surfaces than do mature landforms such as alases and the lakes therein. These findings emphasize the high potential of young thermokarst lakes in CY to rapidly mobilize old, mobile carbon from ice-rich permafrost deposits. They also highlight the necessity to understand the different stages of thermokarst lake evolution and changes because these influence not only local and regional hydrology and human living conditions but also biogeochemical cycles.

6. Conclusion

We used satellite and historical airborne imagery as well as high-resolution topographical data to map and analyze the differences in thermokarst lake sizes and evolution in the continuous permafrost regions of CY, Russia. Statistical analyses of climatic and environmental data were also applied to analyze and compare the driving factors underlying variations of older lakes within alas basins and younger lakes on yedoma uplands. It was shown that young thermokarst lakes have been rapidly evolving on yedoma uplands during the last 70 years. The thermokarst activity was mainly initiated by the anthropogenic destruction of the forest cover, and increased in particular during the last two decades due to changing climatic and permafrost conditions. The area of residual lakes within alas basins oscillates with changing climatic conditions, but comparatively larger catchment areas and subsurface hydrological conditions could have played an important role, too. Statistical analyses of long-term climatic data show that winter precipitation and winter temperatures as well as active-layer properties are the main factors controlling the water balance of both kinds of lakes, but summer weather and permafrost conditions additionally influence yedoma-lake growth. Regionally, lake sizes and distribution differ in relation to the diverse geomorphological, cryolithological, and hydrological conditions of different ice-complex terraces in the Lena-Aldan interfluvium region. Increasing thermokarst activity is currently linked, in particular, to older terraces with higher ground-ice contents. Given climate projections that forecast increases in precipitation and temperatures in CY, our study reveals that thermokarst activity will likely stay at a high level and wet conditions will probably persist within alas basins in the near future. However, our results also highlight the complex interplay of geomorphological factors, permafrost properties, anthropogenic influences, and climatic conditions that influence thermokarst processes and suggest that it is always important to consider the different types and origins of lakes and landforms in permafrost regions. Understanding permafrost dynamics and thermokarst processes is particularly important in the case of the populated region of CY due to this region's thick ice-rich permafrost that is highly vulnerable to climate changes, and to the socio-economic consequences of changing permafrost.

Acknowledgments

This research was funded by the German Research Foundation (DFG UL426/1-1). We greatly appreciate the efforts of all Russian and German colleagues in organizing and supporting the field work and lab analyses. We thank, in particular, Julia Boike, Alexey R. Desyatkin, Avksenty Kondakov, Johannes Schmidt, Christian Siegert, Christine Siegert, and Peter V. Efremov for field assistance and/or discussions during earlier phases of this work. The paper benefited by English proof-reading and valuable comments from Candace S. O'Connor (Scientific Editor, Fairbanks, Alaska). We are also very thankful for valuable comments and constructive reviews by three anonymous referees and L.S. Shirokova. AlosPrism data were kindly provided by JAXA and ESA through the LEDAM project (awarded by ESA ADEN, PI H. Lantuit, ID 3616). Pleiades data were provided to M. Ulrich through the Astrium GEO Initiative-Planet Action project-Russia 9809. Russian historical airborne images were used with the friendly permission of the Melnikov Permafrost Institute, SB RAS, Yakutsk, Russia. All data for this paper are properly cited and referenced in the reference list. Data may be available upon request to the corresponding author.

References

- Aré, F. E. (1969), Temperature regime of the Central Yakutian lakes in the springtime [in Russian], in *Questions of the Geography of Yakutia* No. 5, edited by M. K. Gavrilova, pp. 73–77, Yakut Book Publ., Yakutsk, Russia.
- Arp, C. D., B. M. Jones, A. K. Liljedahl, K. M. Hinkel, and J. A. Welker (2015), Depth, ice thickness, and ice-out timing cause divergent hydrologic responses among Arctic lakes, *Water Resour. Res.*, 51, 9379–9401, doi:10.1002/2015WR017362.
- Boike, J., T. Grau, B. Heim, F. Günther, M. Langer, S. Muster, I. Gouttevin, and S. Lange (2016), Satellite-derived changes in the permafrost landscapes of Central Yakutia, 2000–2011: Wetting, drying, and fires, *Global Planet. Change*, 139, 116–127, doi:10.1016/j.gloplacha.2016.01.001.
- Bosikov, N. P. (1998), Wetness variability and dynamics of thermokarst processes in Central Yakutia, in *Proceedings of the 7th International Permafrost Conference*, edited by A. G. Lewkowicz and M. Allard, pp. 71–74, Yellowknife, Canada.
- Bosikov, N. P., and M. S. Ivanov (1978), *Geocryological Conditions in the Mountain Ranges and Plains of Asia [in Russian]*, edited by I. A. Nekrasov and I. V. Klimovskii, pp. 113–118, Inst. Merzolotovedeniia SO AN SSSR, Yakutsk, Russia.

- Bring, A., I. Fedorova, Y. Dibike, L. Hinzman, J. Mård, S. H. Mernild, T. Prowse, O. Semenova, S. L. Stuefer, and M.-K. Woo (2016), Arctic terrestrial hydrology: A synthesis of processes, regional effects, and research challenges, *J. Geophys. Res. Biogeosci.*, *121*, 621–649, doi:10.1002/2015JG003131.
- Brouchkov, A., M. Fukuda, A. Fedorov, P. Konstantinov, and G. Iwahana (2004), Thermokarst as a short-term permafrost disturbance, Central Yakutia, *Permafrost Periglacial Processes*, *15*, 81–87, doi:10.1002/ppp.473.
- Chander, G., B. L. Markham, and D. L. Helder (2009), Summary of current radiometric calibration coefficients for Landsat MSS, TM, ETM+, and EO-1 ALI sensors, *Remote Sens. Environ.*, *113*(5), 893–903, doi:10.1016/j.rse.2009.01.007.
- Chen, M., J. C. Rowland, C. J. Wilson, G. L. Altmann, and S. P. Brumby (2014), Temporal and spatial pattern of thermokarst lake area changes at the Yukon Flats, Alaska, *Hydrol. Processes*, *28*, 837–852, doi:10.1002/hyp.9642.
- Crate, S. (2008), Gone the bull of winter? Grappling with the cultural implications of and anthropology's role(s) in global climate change, *Curr. Anthropol.*, *49*(4), 569–595, doi:10.1086/529543.
- Crate, S. (2011), A political ecology of water in mind: Attributing perceptions in the era of global climate change, *Weather Clim. Soc.*, *3*, 148–164, doi:10.1175/WCAS-D-10-05006.1.
- Desyatkin, A. R., F. Takakai, P. P. Fedorov, M. C. Nikolaeva, R. V. Desyatkin, and R. Hatano (2009), CH₄ emission from different stages of thermokarst formation in Central Yakutia, *Soil Sci. Plant Nutr.*, *55*, 558–570, doi:10.1111/j.1747-0765.2009.00389.x.
- Desyatkin, R. V. (2004), Water resources of the taiga-alas landscapes in Central Yakutia and problems of water supply for the population, Proceedings of The 6th International Study Conference on GEWEX in Asia and GAME, edited by J. Matsumoto et al., Publication ID: T7PHV30Jul04165014, Kyoto, Japan.
- Desyatkin, R. V. (2008), *Soil formation in Thermokarst Depressions–Alases of Cryolithozone* [in Russian], Novosibirsk “Nauka”, Novosibirsk, Russia.
- Fedorov, A. N., and P. Y. Konstantinov (2003), Observation of surface dynamics with thermokarst initiation, Yukechi site, CY, in *Permafrost: Proceedings of the 8th International Conference on Permafrost*, edited by W. Haeberli and D. Brandova, pp. 239–243, Univ. of Zürich, Zürich, Switzerland.
- Fedorov, A. N., and P. Y. Konstantinov (2008), Recent changes in ground temperature and the effect on permafrost landscapes in CY, in *Proceedings of the Ninth International Conference on Permafrost*, edited by D. L. Kane and K. M. Hinkel, pp. 433–438, Inst. of Northern Eng., Univ. of Alaska, Fairbanks.
- Fedorov, A. N., and P. Y. Konstantinov (2009), Response of permafrost landscapes of Central Yakutia to current changes of climate, and anthropogenic impacts, *Geogr. Nat. Resour.*, *30*, 146–150.
- Fedorov, A. N., P. P. Gavriliev, P. Y. Konstantinov, T. Hiyama, Y. Iijima, and G. Iwahana (2014a), Estimating the water balance of a thermokarst lake in the middle of the Lena River basin, eastern Siberia, *Ecohydrology*, *7*(2), 188–196, doi:10.1002/eco.1378.
- Fedorov, A. N., R. N. Ivanova, H. Park, H., T. Hiyama, and Y. Iijima (2014b), Recent air temperature changes in the permafrost landscapes on northeastern Eurasia, *Polar Sci.*, *8*(2), 114–128, doi:10.1016/j.polar.2014.02.001.
- Grosse, G., V. Romanovsky, K. Walter, A. Morgenstern, H. Lantuit, and S. Zimov (2008), Distribution of thermokarst lakes and ponds at three Yedoma sites in Siberia, in *Proceedings of the Ninth International Conference on Permafrost*, edited by D. L. Kane and K. M. Hinkel, pp. 551–556, Inst. of Northern Eng., Univ. of Alaska, Fairbanks.
- Grosse, G., B. Jones, and C. Arp (2013), Thermokarst Lakes, drainage, and drained basins, in *Treatise on Geomorphology*, edited by J. F. Shroder, pp. 325–353, Academic, San Diego, Calif.
- Hutchinson, M. F. (1989), A new procedure for gridding elevation and stream line data with automatic removal of spurious pits, *J. Hydrol.*, *106*, 211–232, doi:10.1016/0022-1694(89)90073-5.
- Iijima, Y., A. N. Fedorov, H. Park, K. Suzuki, H. Yabuki, T. C. Maximov, and T. Ohta (2010), Abrupt increases in soil temperatures following increased precipitation in a permafrost region, Central Lena river basin, Russia, *Permafrost Periglacial Processes*, *21*, 30–41, doi:10.1002/ppp.662.
- Iijima, Y., T. Ohta, A. Kotani, A. N. Fedorov, Y. Kodama, and T. C. Maximov (2014), Sap flow changes in relation to permafrost degradation under increasing precipitation in an eastern Siberian larch forest, *Ecohydrology*, *7*, 177–187, doi:10.1002/eco.1366.
- Iijima, Y., T. Nakamura, P. Hotaek, Y. Tachibana, and A. N. Fedorov (2016), Enhancement of Arctic storm activity in relation to permafrost degradation in eastern Siberia, *Int. J. Clim.*, *36*, 4265–4275, doi:10.1002/joc.4629.
- IPCC (Intergovernmental Panel on Climate Change) (2013), in *Climate Change 2013: The Physical Science Basis. Contribution Working Group I to the Fifth Assessment Report of the Intergovernmental Panel on Climate Change*, edited by T. F. Stocker et al., pp. 3–29, Cambridge Univ. Press, Cambridge, U. K.
- Iwahana, G., T. Machimura, Y. Kobayashi, A. N. Fedorov, P. Y. Konstantinov, and M. Fukuda (2005), Influence of forest clear-cutting on the thermal and hydrological regime of the active layer near Yakutsk, eastern Siberia, *J. Geophys. Res.*, *110*, G02004, doi:10.1029/2005JG000039.
- Jones, B. M., C. D. Arp, K. M. Hinkel, R. A. Beck, J. A. Schmutz, and B. Winston (2009), Arctic lake physical processes and regimes with implications for winter water availability and management in the National Petroleum Reserve Alaska, *Environ. Manage.*, *43*, 1071–1084.
- Jones, B. M., G. Grosse, C. D. Arp, M. C. Jones, K. M. Walter Anthony, and V. E. Romanovsky (2011), Modern thermokarst lake dynamics in the continuous permafrost zone, northern Seward Peninsula, Alaska, *J. Geophys. Res.*, *116*, G00M03, doi:10.1029/2011JG001666.
- Kessler, M. A., L. J. Plug, and K. M. Walter Anthony (2012), Simulating the decadal- to millennial-scale dynamics of morphology and sequestered carbon mobilization of two thermokarst lakes in NW Alaska, *J. Geophys. Res.*, *117*, G00M06, doi:10.1029/2011JG001796.
- Kokelj, S. V., T. C. Lantz, J. Kanigan, S. L. Smith, and R. Coutts (2009), Origin and polycyclic behavior of tundra thaw slumps, Mackenzie Delta Region, Northwest Territories Canada, *Permafrost Periglacial Processes*, *20*, 173–184, doi:10.1002/ppp.642.
- Kravtsova, V., and T. Tarasenko (2011), The dynamics of thermokarst lakes under climate changes since 1950, Central Yakutia, *Kriosfera Zemli*, *15*(3), 31–42.
- Kravtsova, V. I., and A. G. Bystrova (2009), Changes in thermokarst lake sizes in different regions of Russia for the last 30 years [in Russian], *Kriosfera Zemli*, *13*(2), 16–42.
- Labrecque, S., D. Lacelle, C. R. Duguay, B. Lauriol, and J. Hawkings (2009), Contemporary (1951–2001) evolution of lakes in the Old Crow Basin, Northern Yukon, Canada: Remote sensing, numerical modeling, and stable isotope analysis, *Arctic*, *62*(2), 225–238.
- Lantz, T. C., and K. W. Turner (2015), Changes in lake area in response to thermokarst processes and climate in Old Crow Flats, Yukon, *J. Geophys. Res. Biogeosci.*, *120*, 513–524, doi:10.1002/2014JG002744.
- Lara, M. J., H. Genet, A. D. McGuire, E. S. Euskirchen, Y. Zhang, D. R. N. Brown, M. T. Jorgenson, V. E. Romanovsky, A. Breen, and W. R. Bolton (2016), Thermokarst rates intensify due to climate change and forest fragmentation in an Alaskan boreal forest lowland, *Global Change Biol.*, *22*, 816–829, doi:10.1111/gcb.13124.

- Ling, F., and T. Zhang (2003), Impact of the timing and duration of seasonal snow cover on the active layer and permafrost in the Alaskan Arctic, *Permafrost Periglacial Processes*, *14*, 141–150.
- Mészáros, C. (2012), The Alaas: Cattle economy and environmental perception of sedentary Sakhas in Central Yakutia, *Sibirica*, *11*(2), 1–34.
- Mirkin, B. M., P. A. Gogoleva, and K. E. Konoenov (1985), The vegetation of Central Yakutian alases, *Folia Geobot. Phytotax.*, *20*, 345–395.
- Morgenstern, A., G. Grosse, F. Günther, I. Fedorova, and L. Schirmermeister (2011), Spatial analyses of thermokarst lakes and basins in Yedoma landscapes of the Lena Delta, *Cryosphere*, *5*, 849–867, doi:10.5194/tc-5-849-2011.
- Muster, S., B. Heim, A. Abnizova, J. Boike (2013), Water body distributions across scales: A remote sensing based comparison of three Arctic Tundra wetlands, *Remote Sens.*, *5*, 1498–1523, doi:10.3390/rs5041498.
- NOAA/NCDC (2015), *GHCND (Global Historical Climatology Network)-Monthly Summaries From Jakutsk (Station: RSM00024959)*, Boulder, Colo. [Available at <http://www.ncdc.noaa.gov/>, last accessed 1 Jul 2015.]
- Olthof, I., R. H. Fraser, and C. Schmitt (2015), Landsat-based mapping of thermokarst lake dynamics on the Tuktoyaktuk Coastal Plain, Northwest Territories, Canada since 1985, *Remote Sens. Environ.*, *168*, 194–204, doi:10.1016/j.rse.2015.07.001.
- Park, H., Y. Iijima, H. Yabuki, T. Ohta, J. Walsh, Y. Kodama, and T. Ohata (2011), The application of a coupled hydrological and biogeochemical model (CHANGE) for modeling of energy, water, and CO₂ exchanges over larch forest in eastern Siberia. *J. Geophys. Res.*, *116*, D15102, doi:10.1029/2010JD015386.
- Pestryakova, L. A., U. Herzschuh, S. Wetterich, and M. Ulrich (2012), Present-day variability and Holocene dynamics of permafrost-affected lakes in central Yakutia (Eastern Siberia) inferred from diatom records. *Quat. Sci. Rev.*, *51*, 56–70, doi:10.1016/j.quascirev.2012.06.020.
- Plug, L. J., C. Walls, and B. M. Scott (2008), Tundra lake changes from 1978 to 2001 on the Tuktoyaktuk Peninsula, western Canadian Arctic, *Geophys. Res. Lett.*, *35*, L03502, doi:10.1029/2007GL032303.
- Riordan, B., D. Verbyla, and A. D. McGuire (2006), Shrinking ponds in subarctic Alaska based on 1950–2002 remotely sensed images, *J. Geophys. Res.*, *111*, G04002, doi:10.1029/2005JG000150.
- Roach, J., B. Griffith, D. Verbyla, and J. Jones (2011), Mechanisms influencing changes in lake area in Alaskan boreal forest, *Global Change Biol.*, *17*, 2567–2583, doi:10.1111/j.1365-2486.2011.02446.x.
- Romanovsky, V. E., T. S. Sazonova, V. T. Balobaev, N. I. Shender, and D. O. Sergueev (2007), Past and recent changes in air and permafrost temperatures in eastern Siberia, *Global Planet. Change*, *56*(3–4), 399–413, doi:10.1016/j.gloplacha.2006.07.022.
- Santoro, M., and T. Strozzi (2012), *Circumpolar Digital Elevation Models > 55° N With Links to Geotiff Images*, PANGAEA, Earth & Environmental Science, Bremen, Germany, doi:10.1594/PANGAEA.779748.
- Séjourné, A., F. Costard, A. N. Fedorov, J. Gargani, J. Skorve, M. Massé, and D. Mège (2015), Evolution of the banks of thermokarst lakes in Central Yakutia (Central Siberia) due to retrogressive thaw slump activity controlled by insolation. *Geomorphology*, *241*, 31–40, doi:10.1016/j.geomorph.2015.03.033.
- Shur, Y., K. M. Hinkel, and F. E. Nelson (2005), The transient layer: Implications for geocryology and climate-change science. *Permafrost Periglacial Processes*, *16*, 5–17, doi:10.1002/ppp.518.
- Sjöberg, Y., G. Hugelius, and P. Kuhry (2012), Thermokarst lake morphology and erosion features in two peat plateau areas of Northeast European Russia, *Permafrost Periglacial Processes*, *24*(1), 75–81, doi:10.1002/ppp.1762.
- Smith, L. C., Y. Sheng, G. M. MacDonald, and L. D. Hinzman (2005), Disappearing Arctic lakes, *Science*, *308*, 1429, doi:10.1126/science.1108142.
- Soloviev, P. A. (1959), *Cryolithic zone of the Northern Part of Lena-Amga Interfluve* [in Russian], pp. 142, Izdatel'stvo Akademii SSSR, Moscow.
- Soloviev, P. A. (1961), Cyclic variations in the water level of alas lakes in Central Yakutia and their relation to climate element variations (in Russian). *Vopr. Geograf. Yakutii*, *1*, 48–54.
- Soloviev, P. A. (1973), Thermokarst phenomena and landforms due to frost heaving in Central Yakutia, *Biuletyn Peryglacjalny*, *23*, 135–155.
- Tarasenko, T. V. (2013), Interannual variations in the areas of thermokarst lakes in Central Yakutia, *Water Resour.*, *40*(2), 111–119, doi:10.1134/S0097807813010107.
- Ulrich, M., A. Morgenstern, F. Günther, D. Reiss, K. E. Bauch, E. Hauber, S. Rössler, and L. Schirmermeister (2010), Thermokarst in Siberian ice-rich permafrost: Comparison to asymmetric scalloped depressions on Mars, *J. Geophys. Res.*, *115*, E10009, doi:10.1029/2010JE003640.
- Ulrich, M., H. Matthes, Y. Iijima, H. Saito, H. Park, and A. Fedorov (2015), Size, distribution, and evolution of thermokarst lakes in CY, Russia, Abstract GC23J-1222 presented at 2015 AGU Fall Meeting, San Francisco, Calif., doi:10.13140/RG.2.1.2153.4804.
- van Huissteden, J., C. Berrittella, F. J. W. Parmentier, Y. Mi, T. C. Maximov, and A. J. Dolman (2011), Methane emissions from permafrost thaw lakes limited by lake drainage, *Nat. Clim. Change*, *1*, 119–123, doi:10.1038/nclimate1101.
- Walter, K. M., M. E. Edwards, G. Grosse, S. A., Zimov, and F. S. Chapin III (2007), Thermokarst lakes as a source of atmospheric CH₄ during the last deglaciation, *Science*, *318*, 633–636, doi:10.1126/science.1142924.
- West, J. J., and L. J. Plug (2008), Time-dependent morphology of thaw lakes and taliks in deep and shallow ground ice, *J. Geophys. Res.*, *113*, F01009, doi:10.1029/2006JF000696.
- Xu, H. (2006), Modification of normalized difference water index (NDWI) to enhance open water features in remotely sensed imagery, *Int. J. Remote Sens.*, *27*(14), 3025–3033, doi:10.1080/01431160600589179.
- Yoshikawa K., and L. D. Hinzman (2003), Shrinking thermokarst ponds and groundwater dynamics in discontinuous permafrost near Council, Alaska, *Permafrost Periglacial Processes*, *14*, 151–160, doi:10.1002/ppp.451.
- Zhang, T., et al. (2005), Spatiat and temporal variability in active layer thickness over the Russian Arctic drainage basin, *J. Geophys. Res.*, *110*, D16101, doi:10.1029/2004JD005642.